

**Figure 3. Effect of deregulated miRNAs on expression of their target genes.** (A) miR-101 represses *STMN1*. Top: Reintroduction of miR-101 into NKYS cells reduced mRNA levels of *STMN1*. mRNA levels of *STMN1* were determined by quantitative RT-PCR analysis. Cells were transduced by lentivirus produced by miRNA precursor expression vectors or a control vector. Cells were harvested 4 days after transduction. Mature miR-101 transcript was determined by TaqMan miRNA assay. Bottom: 3'-UTR luciferase reporter assay of *STMN1*. The 293T cells were cotransfected with a reporter construct with or without 3'-UTR of *STMN1* that contain 2 potential miR-101 binding sites and an miRNA expression vector with or without hsa-miR-101 precursor sequence. Reporter constructs with point mutations to the seed sequence of either miR-101 target site were similarly cotransfected. Luciferase activity was determined 48 hours after transfection. (B) miR-30b represses *PRDM1*. Top: Reintroduction of miR-30b into NK-YS cells reduced mRNA levels of *PRDM1*. Cells were transiently transfected by miRNA-30b mimics. Expression of *PRDM1* at 48 hours after transfection was determined by quantitative RT-PCR analysis. Bottom: 3'-UTR luciferase reporter assay of *PRDM1*. The 293T cells were cotransfected with a reporter construct with or without the whole 3'-UTR of *PRDM1* cloned to the distal end of the firefly luciferase gene and an miRNA expression vector with or without the hsa-miR-30b precursor sequence. Luciferase activity was determined 48 hours after transfection. (C) Re-expression of miR-101, miR-26a, or miR-26b in NK-YS cells reduced expression of *BCL-2*. Cells were transduced by lentivirus produced by miRNA precursor expression vectors or a control vector and were harvested 4 days after transduction for quantitative RT-PCR analysis.

### Downstream pathways affected by dysregulated miRNA

Although previously thought to mediate mainly the inhibition of protein translation, recent studies suggest that miRNAs also extensively down-regulate mRNA expression through mRNA decay.<sup>16</sup> We therefore correlated the expression of predicted target genes using data from our previous GEP study<sup>3</sup> with the expression of the dysregulated miRNA and identified a total of 226 target genes whose gene expressions were inversely correlated with the expression of the 41 deregulated miRNA (supplemental Figure 3). It is apparent that some miRNAs, such as miR-30b, miR-15a, let-7a, let-7c, and let-7a, regulate multiple target genes, whereas others have only one specific target gene. Conversely, some target genes (eg, *E2F7* and *EZH2*) are regulated by multiple miRNAs, whereas others are regulated by a single miRNA.

There is a significant enrichment among these predicted target genes for genes involved in cell cycle-related pathways, MAPK and p53 signaling pathways (Table 2). This is consistent with our previous findings showing increased expression of cell cycle-related genes and activation of p53 pathway in NKTL.<sup>3</sup>

### IHC reveals overexpression of target proteins of suppressed miRNAs in NKTL

To further validate our gene expression results, we performed IHC for selected target proteins of the deregulated miRNAs in NKTL, including MUM1/IRF4, BLIMP1, and STMN1 on TMA sections containing 33 samples of NKTL and whole paraffin sections of 5 cases that were not included in the TMAs. In corroboration with the MEP findings, we observed a significant percentage of our NKTL cases showing positive expression for MUM1/IRF4 (20 of 38, 53%), BLIMP1 (17 of 34, 50%), and STMN1 (20 of 35, 57%; Figure 4A-B; supplemental Table 6A). In contrast, normal NK cells

show minimal ( $\leq 5\%$ ) to absent expression of the 3 target proteins (supplemental Table 6B). Similarly, these proteins were aberrantly expressed in NKTL cell lines (supplemental Figure 4). In addition, cases with greater percentage ( $> 10\%$ ) of positive staining cells for the 3 proteins, had higher expression of the corresponding mRNA (Figure 4C). The expression of these mRNAs is also significantly inversely correlated with the expression of their regulating miRNAs (supplemental Figure 3), further suggesting that the overexpression of MUM1, BLIMP1, and STMN1 in NKTL may be driven by abnormal expression of their regulating miRNAs.

### Mechanism of miRNA dysregulated in NKTL

Next, we investigated the possible mechanisms of miRNA dysregulation in NKTL. A number of the dysregulated miRNAs are located within host gene sequences. However, only 3 miRNAs, miR-152, miR-598, and miR-378, have correlated expression with their host genes. The regulation of these miRNA and gene expression is not associated with known deletion or amplification of the genomic locus based on a previous publication of array comparative genomic hybridization analysis.<sup>17</sup> Two underexpressed miRNAs, miR-186 and miR-101, are located within a genomic locus that is commonly deleted in NKTL, chromosome 1p21.3-p31.2 (Table 3).<sup>17</sup> The miRNA signature of NKTL from our analysis is one associated with mainly down-regulation of miRNAs. Recently, it has been shown that MYC can cause extensive repression of miRNA expression.<sup>18</sup> Indeed, in our cohort, tumor samples with increased expression of BLIMP1, MUM1, and STMN1 proteins, regulated by their underexpressed miRNAs, showed higher MYC nuclear expression, consistent with MYC activation (Figure 4B). EBV infection is universal in NKTL. Indeed, 4 of the deregulated

**Table 2. Enriched KEGG pathways among predicted gene targets of deregulated miRNAs in NKTL**

| KEGGID | P      | Odds ratio  | Count | Size | Term   | Genes   |
|--------|--------|-------------|-------|------|--|---|
| 770    | .00005 | 22.96432681 | 4     | 15   | Pantothenate and CoA biosynthesis            | BCAT1, BCAT2, PANK1, PANK3                            |
| 290    | .00044 | 23.4        | 3     | 11   | Valine, leucine, and isoleucine biosynthesis | BCAT1, BCAT2, IARS                                    |
| 4115   | .00055 | 6.206116464 | 6     | 68   | p53 signaling pathway                        | CASP3, CCNE1, CHEK1, IGF1, CCNE2, BBC3                |
| 4110   | .00057 | 4.531014493 | 8     | 123  | Cell cycle                                   | CCNE1, CDC25A, CHEK1, MAD2L1, TFDP1, TTK, WEE1, CCNE2 |
| 4114   | .00155 | 4.293859649 | 7     | 112  | Oocyte meiosis                               | ADCY3, ADCY8, CCNE1, IGF1, IGF1R, MAD2L1, CCNE2       |
| 4914   | .00175 | 4.853855006 | 6     | 85   | Progesterone-mediated oocyte maturation      | ADCY3, ADCY8, CDC25A, IGF1, IGF1R, MAD2L1             |
| 5215   | .00945 | 3.844590369 | 5     | 87   | Prostate cancer                              | BCL2, CCNE1, IGF1, IGF1R, CCNE2                       |
| 4510   | .00994 | 2.730212766 | 8     | 196  | Focal adhesion                               | BCL2, CDC42, ELK1, IGF1, IGF1R, MYLK, VEGFA, TLN2     |
| 4912   | .01513 | 3.38227185  | 5     | 98   | GnRH signaling pathway                       | ADCY3, ADCY8, CDC42, HBEGF, ELK1                      |
| 4614   | .02164 | 8.205761317 | 2     | 17   | Renin-angiotensin system                     | ENPEP, NLN  |
| 5210   | .03373 | 3.113924051 | 4     | 84   | Colorectal cancer                            | BCL2, CASP3, IGF1R, ACVR1C                            |
| 4150   | .03533 | 3.868 75    | 3     | 51   | mTOR signaling pathway                       | IGF1, VEGFA, DDIT4                                    |
| 5414   | .03884 | 2.963230862 | 4     | 88   | Dilated cardiomyopathy                       | ADCY3, ADCY8, ATP2A2, IGF1                            |
| 4010   | .04517 | 1.984836601 | 8     | 263  | MAPK signaling pathway                       | CASP3, CDC42, DUSP4, ELK1, FGF7, STMN1, NTRK2, ACVR1C |
| 52     | .04708 | 5.119341564 | 2     | 26   | Galactose metabolism                         | GCK, B4GALT2  |
| 450    | .04708 | 5.119341564 | 2     | 26   | Seleno amino acid metabolism                 | AHCY, CTH   |

miRNAs that we observed have been reported to be down-regulated (let 7g, let-7 and let-7c)<sup>19</sup> and up-regulated (miR-155)<sup>20</sup> on EBV infection (Table 3), suggesting that EBV infection may also have an effect on miRNA deregulation in NKTL.

## Discussion

NKTL is a highly aggressive tumor, and a better understanding of the molecular abnormalities underlying this condition will provide important insights into the biology of this disease and potential new therapeutic avenues. To the best of our knowledge, this is the first comprehensive genome-wide study of miRNA expression profiling using the microarray platform on FFPE NKTL samples. The validity of our results was supported by quantitative PCR validation as well as corroboration of our *in silico* functional analysis with IHC in a larger dataset, showing good correlation between MEP, GEP, IHC, and RT-PCR results. In the present study, we characterized the miRNA signature of NKTL compared with normal NK cells. Our results identified the dysregulated miRNAs in NKTL, target genes involved, and activation of signaling pathways that may be relevant to the pathophysiology of the disease and could potentially serve as therapeutic targets.

We found that the predominant changes are down-regulation of miRNAs. We validated that the expression of a number of these down-regulated miRNAs, such as miR-101, miR-26a, miR26b, miR-30b, miR-28-5, and miR-363, affects growth of the NK-YS cell line. In addition, they modulated the expression of their predicted target genes, suggesting that these miRNAs are of functional relevance, and their suppression could lead to increased expression of a number of genes implicated in oncogenesis. Indeed, we confirmed, for the first time, that miR-101 directly regulate *STMN1*.

A recent study by Paik et al reported that miRNA-146a is down-regulated in NKTL and may function as a tumor suppressor in NK/T-cell lymphoma.<sup>21</sup> In line with this study, we also detected down-regulation of miR-146a in FFPE NKTL compared with normal NK cells but not between NK cell lines and normal NK cells (see supplemental Tables 4 and 5). Only 2 miRNAs (miR-155 and miR-378) were up-regulated in both NKTL and NK cell lines compared with normal NK cells. Overexpression of miR-155 induced activation of AKT signaling pathway in NK cell lymphoma,<sup>7</sup> whereas overexpression of *miR-378* has been found to enhance cell survival, reduce caspase-3 activity, and promote tumor growth and angiogenesis.<sup>22</sup> In corroboration with data from GEP studies in NKTL, targets of dysregulated miRNA in NKTL are

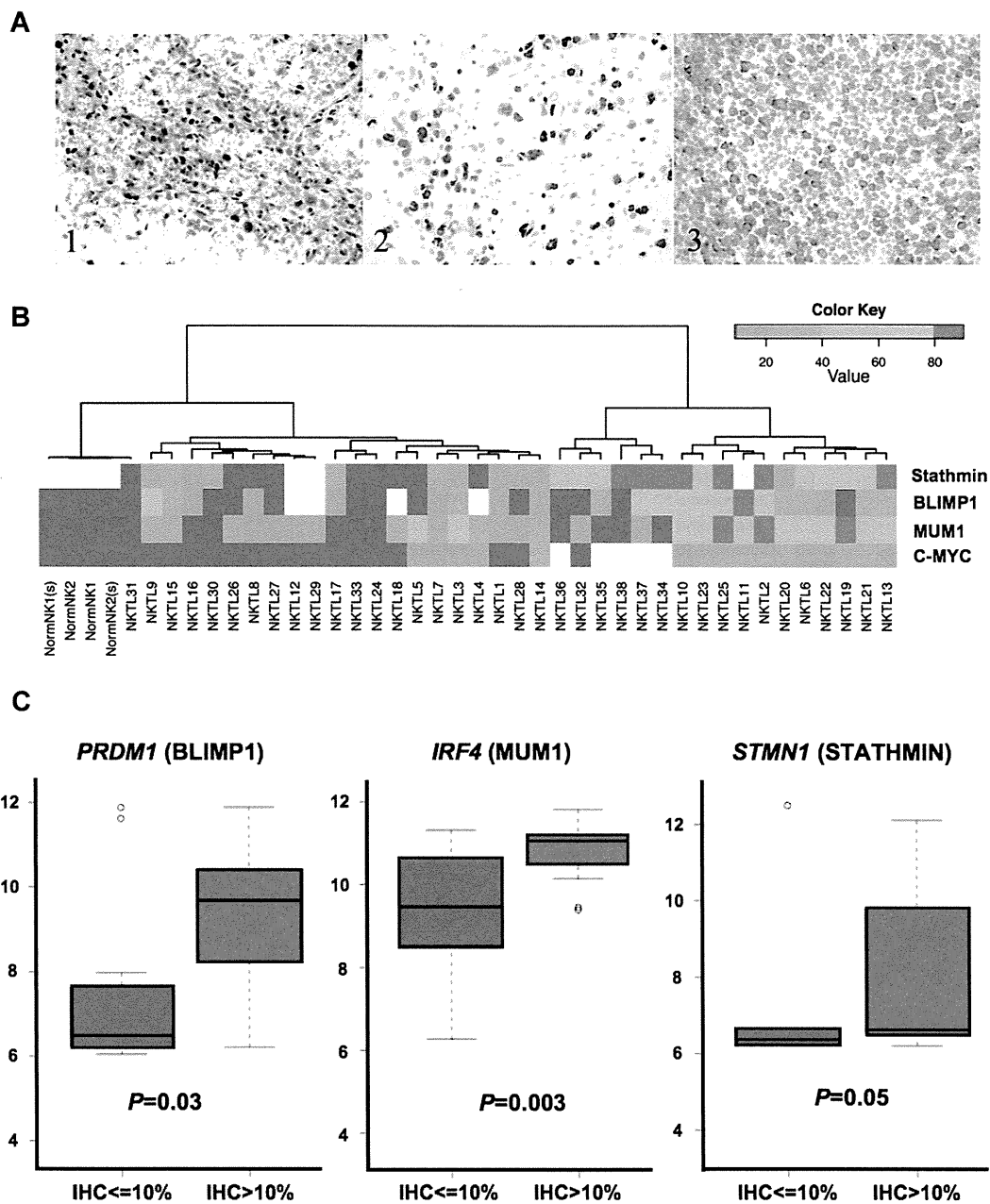


**Figure 4. Expression of protein targets of deregulated miRNA.** (A) IHC showing overexpression of (i) BLIMP1, (ii) MUM1, and (iii) STATHMIN in the tumor cells. BLIMP1 and MUM1 are expressed in the nuclei, whereas STATHMIN is expressed in the cytoplasm of the neoplastic lymphoid cells. All photographs were taken with a DP20 Olympus camera (Olympus) using an Olympus BX41 microscope (Olympus); images were acquired using DP Controller 2002 (Olympus) and processed using Adobe Photoshop Version 7.0 (Adobe Systems). Original magnifications  $\times 600$ . (B) The percentage of tumor cells staining for the different protein markers are represented in the form of a heat map. The color scale corresponding to the percentage of positive staining cells is appended in the left upper corner. Samples with results represented by white indicate that the stain was not done because of inadequate material. Cases with the highest expression of STATHMIN, MUM1, and BLIMP1 also have the highest expression of MYC. (C) The expression of mRNA corresponding to these proteins was higher in those samples where  $> 10\%$  of tumor cells are staining positive for each protein marker. For BLIMP1 and MUM1, it is statistically significant.

significantly enriched for genes involved in the cell cycle-related pathway, p53 pathway, and MAPK signaling pathway.<sup>1-3</sup> This suggests that oncogenic pathways activated in NKTL may be in part mediated by miRNA dysregulation.

BLIMP1 and MUM1/IRF4, 2 of the up-regulated targets identified in this study with corresponding protein overexpression, are of interest as they have been previously implicated in T- and NK-cell malignancies.<sup>23</sup> Our study reveals that the up-regulation of BLIMP1 and IRF4 in NKTL may be driven by the suppression of their regulating miRNAs. Besides being a master regulator of terminal B-cell differentiation, BLIMP-1 also plays a role in the

later stages of T-cell differentiation.<sup>24,25</sup> Recently, BLIMP1 was shown to be required for NK-cell maturation and for regulating their proliferative potential.<sup>26</sup> We found that BLIMP1 expression is significantly higher and aberrant in a subset of NKTL compared with normal NK cells. Expression of BLIMP1 is also associated with chemoresistance and poorer disease outcome in T-cell malignancies. The multiple myeloma oncogene-1 (MUM1/IRF4) encodes a transcription factor thought to play a central role in the development of lymphoid cells. Besides being expressed in B cells and plasma cells, IRF4 is known to be expressed in activated T-cell malignancies and to regulate T-cell transformation. Expression of

**Table 3. Potential mechanisms of miRNA deregulation in NKTL**

| Dysregulated miRNA | Dysregulated in NKTL | Genomic loci  | Affected by EBV infection | Host gene  | Correlation with host gene expression | Abnormality in genomic loci | aCGH band    |
|--------------------|----------------------|---------------|---------------------------|------------|---------------------------------------|-----------------------------|--------------|
| hsa-miR-342-5p     | –                    | Chromosome 14 |                           | EVL        |                                       |                             |              |
| hsa-miR-26b        | –                    | Chromosome 2  |                           | CTDSP1     |                                       |                             |              |
| hsa-miR-363        | –                    | Chromosome X  |                           |            |                                       |                             |              |
| hsa-miR-150        | –                    | Chromosome 19 |                           |            |                                       |                             |              |
| hsa-miR-28-5p      | –                    | Chromosome 3  |                           | LPP        |                                       |                             |              |
| hsa-miR-152        | –                    | Chromosome 17 | +                         | COPZ2      | Yes                                   |                             |              |
| hsa-miR-361-3p     | –                    | Chromosome X  |                           | CHM        |                                       |                             |              |
| hsa-miR-22*        | –                    | Chromosome 17 |                           | C17orf91   |                                       |                             |              |
| hsa-miR-340        | –                    | Chromosome 5  |                           | RNF130     |                                       |                             |              |
| hsa-miR-598        | –                    | Chromosome 8  |                           | XKR6       | Yes                                   |                             |              |
| hsa-miR-181a-2*    | –                    | Chromosome 9  |                           | NR6A1      |                                       |                             |              |
| hsa-miR-132        | –                    | Chromosome 17 |                           |            |                                       |                             |              |
| hsa-miR-194        | –                    | Chromosome 1  |                           | IARS2      |                                       |                             |              |
| hsa-miR-768-3p     | –                    | Chromosome 16 |                           | AP1G1      |                                       |                             |              |
| hsa-miR-873        | –                    | Chromosome 9  |                           |            |                                       |                             |              |
| hsa-miR-338-3p     | –                    | Chromosome 17 |                           | AATK       |                                       |                             |              |
| hsa-miR-215        | –                    | Chromosome 1  |                           | IARS2      |                                       |                             |              |
| hsa-miR-186        | –                    | Chromosome 1  |                           | ZRANB2     |                                       | –                           | 1p21.3-p31.2 |
| hsa-miR-140-3p     | –                    | Chromosome 16 |                           | WWP2       |                                       |                             |              |
| hsa-miR-140-5p     | –                    | Chromosome 16 |                           | WWP2       |                                       |                             |              |
| hsa-miR-374b       | –                    | Chromosome X  |                           | NCRNA00182 |                                       |                             |              |
| hsa-miR-26a        | –                    | Chromosome 12 |                           | CTDSP2     |                                       |                             |              |
| hsa-let-7g         | –                    | Chromosome 3  | –                         | WDR82      |                                       |                             |              |
| hsa-miR-342-3p     | –                    | Chromosome 14 |                           | EVL        |                                       |                             |              |
| hsa-miR-101        | –                    | Chromosome 1  |                           |            |                                       | –                           | 1p21.3-p31.2 |
| hsa-miR-192        | –                    | Chromosome 11 |                           |            |                                       |                             |              |
| hsa-miR-374a       | –                    | Chromosome X  |                           | NCRNA00182 |                                       |                             |              |
| hsa-miR-876-5p     | –                    | Chromosome 9  |                           |            |                                       |                             |              |
| hsa-miR-22         | –                    | Chromosome 17 |                           | C17orf91   |                                       |                             |              |
| hsa-miR-10a        | –                    | Chromosome 17 |                           |            |                                       |                             |              |
| hsa-miR-590-5p     | –                    | Chromosome 7  |                           | EIF4H      |                                       |                             |              |
| hsa-miR-30b        | –                    | Chromosome 8  |                           |            |                                       |                             |              |
| hsa-miR-181c       | –                    | Chromosome 19 |                           |            |                                       |                             |              |
| hsa-miR-142-5p     | –                    | Chromosome 17 |                           |            |                                       |                             |              |
| hsa-let-7a         | –                    | Chromosome 11 | –                         | LOC399959  |                                       |                             |              |
| hsa-miR-155        | +                    | Chromosome 21 | +                         | MIR155HG   |                                       |                             |              |
| hsa-let-7c         | –                    | Chromosome 21 | –                         | C21orf34   |                                       |                             |              |
| hsa-miR-378        | +                    | Chromosome 5  |                           | PPARGC1B   | Yes                                   |                             |              |
| hsa-miR-181a       | –                    | Chromosome 1  |                           |            |                                       |                             |              |
| hsa-miR-142-3p     | –                    | Chromosome 17 |                           |            |                                       |                             |              |
| hsa-miR-15a        | –                    | Chromosome 13 |                           | DLEU2      |                                       |                             |              |

– indicates down-regulated; +, upregulated; and empty fields, no abnormalities detected.

IRF4 is also associated with inferior overall survival in peripheral T-cell lymphoma, and this association was observed across PTCL subtypes.<sup>27</sup> Recently, MUM1/IRF4 expression in PTCLs, including NKTL, was linked to expression of BLIMP1. PTCL cell lines treated in vitro with the proteasome inhibitor bortezomib down-regulated MUM1/IRF4, an effect dependent on NF- $\kappa$ B inhibition and associated with BLIMP1 down-regulation.<sup>28</sup> Given that IRF4 overexpression is oncogenic in vitro,<sup>29</sup> and because NKTL lacks good treatment options, MUM1/IRF4 might represent a potential therapeutic target in patients with NKTL.

miRNAs are often encoded in fragile sites in the genome, where their expression can be altered by events, such as genomic amplification, loss of heterozygosity, viral integration, or genomic rearrangement.<sup>30</sup> Our analysis revealed that 5% of the deregulated miRNAs in NKTL correlated with their host gene expression and may be deregulated as a result of abnormalities affecting the host genes. However, except for miR-101 and miR-186, which are

located on 1p21.3-p31.2 that has been previously reported to be deleted in NKTL,<sup>17</sup> chromosomal alteration appears to be an unlikely mechanism contributing to the deregulation of miRNAs in NKTL.

EBV infection has been described to regulate the expression of miRNAs in Burkitt lymphoma.<sup>31</sup> Our results reveal the down-regulation of let-7g, let-7a, and let-7c, and up-regulation of miR-155 in both NK cell lines and FFPE NKTL samples. miRNAs let-7g, let-7a, and let-7c have been demonstrated in other studies to be down-regulated by EBV.<sup>19</sup> Similarly, overexpression of miR-155 has been demonstrated in EBV-infected B lymphocytes displaying type III latency,<sup>20</sup> and this is because of EBV gene expression and not epigenetic differences in cell lines tested.<sup>32</sup> It is plausible that EBV may play a role in the dysregulation of these miRNAs in NKTL. Our result is also consistent with the study by Yamanaka et al, which demonstrated that overexpression of miR-155 resulted in the activation of AKT signaling pathway in NK cell lymphoma.<sup>7</sup>

As most of the dysregulated miRNAs are down-regulated, one important mechanism driving changes in miRNA may be MYC activation, which has been shown to repress a large number of miRNAs in tumor development.<sup>18</sup> We have shown previously that MYC is activated in a substantial number of NKTL,<sup>3</sup> and here we show correlation between MYC activation and overexpression of target proteins of down-regulated miRNA, suggesting that MYC activation may be one of the mechanisms in the deregulation of miRNA in NKTL.

In conclusion, our study indicates that the deregulation of miRNAs is of functional relevance, providing an additional mechanism by which some of the oncogenic pathways may be deregulated and hence contribute to the pathogenesis of NKTL. Furthermore, miRNAs may themselves be potential therapeutic targets that can be exploited in the future.<sup>33,34</sup>

## Acknowledgments

W.-J.C. was supported by the National Medical Research Council Clinician Scientist Investigator Award. This work is supported in part by the Singapore Cancer Syndicate and the Research Center of

Excellence Program (funded by the Singapore National Research Foundation and the Ministry of Education).

## Authorship

Contribution: S.-B.N. designed experiments, performed IHC and scoring, and wrote the manuscript; J.Y. J.L.-S.T., and J.T. performed miRNA functional studies; G.H. performed bioinformatics analysis; V.S. and B.L. performed experiments; C.B. performed microarray experiments; Y.-L.K., N.S., and K.A. provided cell lines and approved the final manuscript; and W.-J.C. designed experiments, performed analysis, and wrote the manuscript.

Conflict-of-interest disclosure: The authors declare no competing financial interests.

Correspondence: Wee-Joo Chng, Department of Haematology-Oncology, National University Hospital, 5 Lower Kent Ridge Road, Main Building, Level 3, Singapore 119074; e-mail: mdccwj@nus.edu.sg; and Siok-Bian Ng, Department of Pathology, National University Hospital, 5 Lower Kent Ridge Road, Main Building, Level 3, Singapore 119074; e-mail: patnsb@nus.edu.sg.

## References

1. Iqbal J, Weisenburger DD, Chowdhury A, et al. Natural killer cell lymphoma shares strikingly similar molecular features with a group of non-hepatosplenic gammadelta T-cell lymphoma and is highly sensitive to a novel aurora kinase A inhibitor in vitro. *Leukemia*. 2011;25(2):348-358.
2. Huang Y, de Reynies A, de Leval L, et al. Gene expression profiling identifies emerging oncogenic pathways operating in extranodal NK/T-cell lymphoma, nasal type. *Blood*. 2010;115(6):1226-1237.
3. Ng SB, Selvarajan V, Huang G, et al. Activated oncogenic pathways and therapeutic targets in extranodal nasal-type NK/T cell lymphoma revealed by gene expression profiling. *J Pathol*. 2011;223(4):496-510.
4. Griffiths-Jones S, Saini HK, van Dongen S, Enright AJ. miRBase: tools for microRNA genomics. *Nucleic Acids Res*. 2008;36(database issue):D154-D158.
5. Bryant A, Lutherborrow M, Ma D. The clinicopathological relevance of microRNA in normal and malignant haematopoiesis. *Pathology*. 2009;41(3):204-213.
6. Farazi TA, Spitzer JL, Morozov P, Tuschl T. miRNAs in human cancer. *J Pathol*. 2011;223(2):102-115.
7. Yamanaka Y, Tagawa H, Takahashi N, et al. Aberrant overexpression of microRNAs activate AKT signaling via down-regulation of tumor suppressors in natural killer-cell lymphoma/leukemia. *Blood*. 2009;114(15):3265-3275.
8. Di Lisio L, Gomez-Lopez G, Sanchez-Beato M, et al. Mantle cell lymphoma: transcriptional regulation by microRNAs. *Leukemia*. 2010;24(7):1335-1342.
9. Xi Y, Nakajima G, Gavin E, et al. Systematic analysis of microRNA expression of RNA extracted from fresh frozen and formalin-fixed paraffin-embedded samples. *RNA*. 2007;13(10):1668-1674.
10. Drexler HG, Fombonne S, Matsuo Y, Hu ZB, Hamaguchi H, Uphoff CC. p53 alterations in human leukemia-lymphoma cell lines: in vitro artifact or prerequisite for cell immortalization? *Leukemia*. 2000;14(1):198-206.
11. Matsuo Y, Drexler HG. Immunoprofiling of cell lines derived from natural killer-cell and natural killer-like T-cell leukemia-lymphoma. *Leuk Res*. 2003;27(10):935-945.
12. Poy MN, Eliasson L, Krutzfeldt J, et al. A pancreatic islet-specific microRNA regulates insulin secretion. *Nature*. 2004;432(7014):226-230.
13. Yekta S, Shih IH, Bartel DP. MicroRNA-directed cleavage of HOXB8 mRNA. *Science*. 2004;304(5670):594-596.
14. Lim LP, Lau NC, Garrett-Engle P, et al. Microarray analysis shows that some microRNAs downregulate large numbers of target mRNAs. *Nature*. 2005;433(7027):769-773.
15. Fehniger TA, Wylie T, Germino E, et al. Next-generation sequencing identifies the natural killer cell microRNA transcriptome. *Genome Res*. 2010;20(11):1590-1604.
16. Huntzinger E, Izaurralde E. Gene silencing by microRNAs: contributions of translational repression and mRNA decay. *Nat Rev Genet*. 2011;12(2):99-110.
17. Iqbal J, Kucuk C, Deleeuw RJ, et al. Genomic analyses reveal global functional alterations that promote tumor growth and novel tumor suppressor genes in natural killer-cell malignancies. *Leukemia*. 2009;23(6):1139-1151.
18. Chang TC, Yu D, Lee YS, et al. Widespread microRNA repression by Myc contributes to tumorigenesis. *Nat Genet*. 2008;40(1):43-50.
19. Godshalk SE, Bhaduri-McIntosh S, Slack FJ. Epstein-Barr virus-mediated dysregulation of human microRNA expression. *Cell Cycle*. 2008;7(22):3595-3600.
20. Jiang J, Lee EJ, Schmittgen TD. Increased expression of microRNA-155 in Epstein-Barr virus transformed lymphoblastoid cell lines. *Genes Chromosomes Cancer*. 2006;45(1):103-106.
21. Paik JH, Jang JY, Jeon YK, et al. MicroRNA-146a downregulates NF-kappaB activity via targeting TRAF6, and functions as a tumor suppressor having strong prognostic implications in NK/T cell lymphoma. *Clin Cancer Res*. 2011;17(14):4761-4771.
22. Lee DY, Deng Z, Wang CH, Yang BB. MicroRNA-378 promotes cell survival, tumor growth, and angiogenesis by targeting SuFu and Fus-1 expression. *Proc Natl Acad Sci U S A*. 2007;104(51):20350-20355.
23. Garcia JF, Roncador G, Sanz AI, et al. PRDM1/BLIMP-1 expression in multiple B and T-cell lymphoma. *Haematologica*. 2006;91(4):467-474.
24. Kallies A, Hawkins ED, Belz GT, et al. Transcriptional repressor Blimp-1 is essential for T cell homeostasis and self-tolerance. *Nat Immunol*. 2006;7(5):466-474.
25. Martins GA, Cimmino L, Shapiro-Shelef M, et al. Transcriptional repressor Blimp-1 regulates T cell homeostasis and function. *Nat Immunol*. 2006;7(5):457-465.
26. Kallies A, Carotta S, Huntington ND, et al. A role for Blimp1 in the transcriptional network controlling natural killer cell maturation. *Blood*. 2011;117(6):1869-1879.
27. Feldman AL, Dogan A, Maurer MJ, et al. Expression of interferon regulatory factor-4 (IRF4/MUM1) is associated with inferior overall survival in peripheral T-cell lymphoma [abstract 140]. 52nd ASH Annual Meeting and Exposition, Orlando FL, December 4-7, 2010.
28. Zhao WL, Liu YY, Zhang QL, et al. PRDM1 is involved in chemoresistance of T-cell lymphoma and down-regulated by the proteasome inhibitor. *Blood*. 2008;111(7):3867-3871.
29. Iida S, Rao PH, Butler M, et al. Deregulation of MUM1/IRF4 by chromosomal translocation in multiple myeloma. *Nat Genet*. 1997;17(2):226-230.
30. Cain GA, Sevnigani C, Dumitru CD, et al. Human microRNA genes are frequently located at fragile sites and genomic regions involved in cancers. *Proc Natl Acad Sci U S A*. 2004;101(9):2999-3004.
31. De Falco G, Antonicelli G, Onnis A, Lazzi S, Bellan C, Leoncini L. Role of EBV in microRNA dysregulation in Burkitt lymphoma. *Semin Cancer Biol*. 2009;19(6):401-406.
32. Yin Q, McBride J, Fewell C, et al. MicroRNA-155 is an Epstein-Barr virus-induced gene that modulates Epstein-Barr virus-regulated gene expression pathways. *J Virol*. 2008;82(11):5295-5306.
33. Bader AG, Brown D, Winkler M. The promise of microRNA replacement therapy. *Cancer Res*. 2010;70(18):7027-7030.
34. Trang P, Weidhaas JB, Slack FJ. MicroRNAs as potential cancer therapeutics. *Oncogene*. 2008;27(suppl 2):S52-S57.

# Novel Mouse Xenograft Models Reveal a Critical Role of CD4<sup>+</sup> T Cells in the Proliferation of EBV-Infected T and NK Cells

Ken-Ichi Imadome<sup>1☯\*</sup>, Misako Yajima<sup>1☯✉</sup>, Ayako Arai<sup>2</sup>, Atsuko Nakazawa<sup>3</sup>, Fuyuko Kawano<sup>1</sup>, Sayumi Ichikawa<sup>1,4</sup>, Norio Shimizu<sup>4</sup>, Naoki Yamamoto<sup>5✉</sup>, Tomohiro Morio<sup>6</sup>, Shouichi Ohga<sup>7</sup>, Hiroyuki Nakamura<sup>1</sup>, Mamoru Ito<sup>8</sup>, Osamu Miura<sup>2</sup>, Jun Komano<sup>5</sup>, Shigeyoshi Fujiwara<sup>1\*</sup>

**1** Department of Infectious Diseases, National Research Institute for Child Health and Development, Tokyo, Japan, **2** Department of Hematology, Tokyo Medical and Dental University, Tokyo, Japan, **3** Department of Pathology, National Center for Child Health and Development, Tokyo, Japan, **4** Department of Virology, Division of Medical Science, Medical Research Institute, Tokyo Medical and Dental University, Tokyo, Japan, **5** AIDS Research Center, National Institute of Infectious Diseases, Tokyo, Japan, **6** Department of Pediatrics and Developmental Biology, Tokyo Medical and Dental University, Tokyo, Japan, **7** Department of Perinatal and Pediatric Medicine, Graduate School of Medical Sciences, Kyushu University, Fukuoka, Japan, **8** Central Institute for Experimental Animals, Kawasaki, Japan

## Abstract

Epstein-Barr virus (EBV), a ubiquitous B-lymphotropic herpesvirus, ectopically infects T or NK cells to cause severe diseases of unknown pathogenesis, including chronic active EBV infection (CAEBV) and EBV-associated hemophagocytic lymphohistiocytosis (EBV-HLH). We developed xenograft models of CAEBV and EBV-HLH by transplanting patients' PBMC to immunodeficient mice of the NOD/Shi-*scid*/IL-2R $\gamma^{\text{null}}$  strain. In these models, EBV-infected T, NK, or B cells proliferated systemically and reproduced histological characteristics of the two diseases. Analysis of the TCR repertoire expression revealed that identical predominant EBV-infected T-cell clones proliferated in patients and corresponding mice transplanted with their PBMC. Expression of the EBV nuclear antigen 1 (EBNA1), the latent membrane protein 1 (LMP1), and LMP2, but not EBNA2, in the engrafted cells is consistent with the latency II program of EBV gene expression known in CAEBV. High levels of human cytokines, including IL-8, IFN- $\gamma$ , and RANTES, were detected in the peripheral blood of the model mice, mirroring hypercytokinemia characteristic to both CAEBV and EBV-HLH. Transplantation of individual immunophenotypic subsets isolated from patients' PBMC as well as that of various combinations of these subsets revealed a critical role of CD4<sup>+</sup> T cells in the engraftment of EBV-infected T and NK cells. In accordance with this finding, *in vivo* depletion of CD4<sup>+</sup> T cells by the administration of the OKT4 antibody following transplantation of PBMC prevented the engraftment of EBV-infected T and NK cells. This is the first report of animal models of CAEBV and EBV-HLH that are expected to be useful tools in the development of novel therapeutic strategies for the treatment of the diseases.

**Citation:** Imadome K-I, Yajima M, Arai A, Nakazawa A, Kawano F, et al. (2011) Novel Mouse Xenograft Models Reveal a Critical Role of CD4<sup>+</sup> T Cells in the Proliferation of EBV-Infected T and NK Cells. *PLoS Pathog* 7(10): e1002326. doi:10.1371/journal.ppat.1002326

**Editor:** Shou-Jiang Gao, University of Texas Health Science Center San Antonio, United States of America

**Received:** January 27, 2011; **Accepted:** September 2, 2011; **Published:** October 20, 2011

**Copyright:** © 2011 Imadome et al. This is an open-access article distributed under the terms of the Creative Commons Attribution License, which permits unrestricted use, distribution, and reproduction in any medium, provided the original author and source are credited.

**Funding:** This study was supported by grants from the Ministry of Health, Labour and Welfare of Japan (H22-Nanchi-080 and H22-AIDS-002), the Grant of National Center for Child Health and Development (22A-9), a grant for the Research on Publicly Essential Drugs and Medical Devices from The Japan Health Sciences Foundation (KHC1014), and the Grant-in-Aid for Scientific Research (C) (H22-22590374). The funders had no role in study design, data collection and analysis, decision to publish, or preparation of the manuscript.

**Competing Interests:** The authors have declared that no competing interests exist.

\* E-mail: imadome@nch.go.jp (KI); shige@nch.go.jp (SF)

✉ Current address: Department of Microbiology, Yong Loo Lin School of Medicine, National University of Singapore, Singapore

☯ These authors contributed equally to this work.

## Introduction

Epstein-Barr virus (EBV) is a ubiquitous  $\gamma$ -herpesvirus that infects more than 90% of the adult population in the world. EBV is occasionally involved in the pathogenesis of malignant tumors, such as Burkitt lymphoma, Hodgkin lymphoma, and nasopharyngeal carcinoma, along with the post-transplantation lymphoproliferative disorders in immunocompromised hosts. Although EBV infection is asymptomatic in most immunologically competent hosts, it sometimes causes infectious mononucleosis (IM), when primarily infecting adolescents and young adults [1]. EBV infects human B cells efficiently *in vitro* and transform them into lymphoblastoid cell lines (LCLs) [2]. Experimental infection of T

and NK cells, in contrast, is practically impossible except in limited conditions [3,4]. Nevertheless, EBV has been consistently demonstrated in T or NK cells proliferating monoclonally or oligoclonally in a group of diseases including chronic active EBV infection (CAEBV) and EBV-associated hemophagocytic lymphohistiocytosis (EBV-HLH) [5,6,7,8,9,10]. CAEBV, largely overlapping the systemic EBV<sup>+</sup> T-cell lymphoproliferative diseases of childhood defined in the WHO classification of lymphomas [11], is characterized by prolonged or relapsing IM-like symptoms, unusual patterns of antibody responses to EBV, and elevated EBV DNA load in the peripheral blood [12,13,14]. CAEBV has a chronic time course with generally poor prognosis; without a proper treatment by hematopoietic stem cell transplantation, the

## Author Summary

Epstein-Barr virus (EBV) is a ubiquitous human herpesvirus that infects more than 90% of the adult human population in the world. EBV usually infects B lymphocytes and does not produce symptoms in infected individuals, but in rare occasions it infects T or NK lymphocytes and causes severe diseases such as chronic active EBV infection (CAEBV) and EBV-associated hemophagocytic lymphohistiocytosis (EBV-HLH). We developed mouse models of these two human diseases in which EBV-infected T or NK lymphocytes proliferate in mouse tissues and reproduce human pathologic conditions such as overproduction of small proteins called "cytokines" that produce inflammatory responses in the body. These mouse models are thought to be very useful for the elucidation of the pathogenesis of CAEBV and EBV-HLH as well as for the development of therapeutic strategies for the treatment of these diseases. Experiments with the models demonstrated that a subset of lymphocytes called CD4-positive lymphocytes are essential for the proliferation of EBV-infected T and NK cells. This result implies that removal of CD4-positive lymphocytes or suppression of their functions may be an effective strategy for the treatment of CAEBV and EBV-HLH.

majority of cases eventually develop malignant lymphoma of T or NK lineages, multi-organ failure, or other life-threatening conditions. Monoclonal or oligoclonal proliferation of EBV-infected T and NK cells, an essential feature of CAEBV, implies its malignant nature, but other characteristics of CAEBV do not necessarily support this notion. For example, EBV-infected T or NK cells freshly isolated from CAEBV patients, as well as established cell lines derived from them, do not have morphological atypia and do not engraft either in nude mice or *scid* mice (Shimizu, N., unpublished results). Clinically, CAEBV has a chronic time course and patients may live for many years without progression of the disease [15]. Although patients with CAEBV do not show signs of explicit immunodeficiency, some of them present a deficiency in NK-cell activity or in EBV-specific T-cell responses, implying a role for subtle immunodeficiency in its pathogenesis [16,17,18].

EBV-HLH is the most common and the severest type of virus-associated HLH and, similar to CAEBV, characterized by monoclonal or oligoclonal proliferation of EBV-infected T (most often CD8<sup>+</sup> T) cells [5,6]. Clinical features of EBV-HLH include high fever, pancytopenia, coagulation abnormalities, hepatosplenomegaly, liver dysfunction, and hemophagocytosis [19]. Overproduction of cytokines by EBV-infected T cells as well as by activated macrophages and T cells reacting to EBV is thought to play a central role in the pathogenesis [20]. Although EBV-HLH is an aggressive disease requiring intensive clinical interventions, it may be cured, in contrast to CAEBV, by proper treatment with immunomodulating drugs [21]. No appropriate animal models have been so far developed for either CAEBV or EBV-HLH.

NOD/Shi-*scid*/IL-2R $\gamma^{\text{null}}$  (referred here as NOG) is a highly immunodeficient mouse strain totally lacking T, B, and NK lymphocytes, and transplantation of human hematopoietic stem cells to NOG mice results in reconstitution of human immune system components, including T, B, NK cells, dendritic cells, and macrophages [22,23]. These so called humanized mice have been utilized as animal models for the infection of certain human viruses targeting the hemato-immune system, including human immunodeficiency virus 1 (HIV-1) and EBV [24,25,26,27,28,29,30]. Xeno-

transplantation of human tumor cells to NOG mice also provided model systems for several hematologic malignancies [31,32,33]. To facilitate investigations on the pathogenesis of CAEBV and EBV-HLH and assist the development of novel therapeutic strategies, we generated mouse models of these two EBV-associated diseases by transplanting NOG mice with PBMC isolated from patients with the diseases. In these models, EBV-infected T, NK, or B cells engrafted in NOG mice and reproduced lymphoproliferative disorder similar to either CAEBV or EBV-HLH. Further experiments with the models revealed a critical role of CD4<sup>+</sup> T cells in the *in vivo* proliferation of EBV-infected T and NK cells.

## Results

### Engraftment of EBV-infected T and NK cells in NOG mice following xenotransplantation with PBMC of CAEBV patients

Depending on the immunophenotypic subset in which EBV causes lymphoproliferation, CAEBV is classified into the T-cell and NK-cell types, with the former being further divided into the CD4, CD8, and  $\gamma\delta$ T types. The nine patients with CAEBV examined in this study are characterized in Table 1 and include all these four types. Intravenous injection of  $1-4 \times 10^6$  PBMC isolated from these nine patients resulted in successful engraftment of EBV-infected T or NK cells in NOG mice in a reproducible manner (Table 1). The results with the patient 1 (CD4 type), patient 3 (CD8 type), patient 5 ( $\gamma\delta$ T type), and patient 9 (NK type) are shown in Figure 1. Seven to nine weeks post-transplantation, EBV DNA was detected in the peripheral blood of recipient mice and reached the levels of  $10^2-10^8$  copies/ $\mu$ g DNA (Figure 1A). By contrast, no engraftment of EBV-infected cells was observed when immunophenotypic fractions containing EBV DNA were isolated from PBMC and injected to NOG mice (Figure 1A and Table 2). An exception was the CD4<sup>+</sup> T-cell fraction isolated from patients with the CD4 type CAEBV, that reproducibly engrafted when transplanted without other components of PBMC (Figure 1A, Table 2). Flow cytometry revealed that the major population of engrafted cells was either CD4<sup>+</sup>, CD8<sup>+</sup>, TCR $\gamma\delta$ or CD16<sup>+</sup>CD56<sup>+</sup>, depending on the type of the donor CAEBV patient (Figure 1B). EBV-infected cells of identical immunophenotypes were found in the patients and the corresponding mice that received their respective PBMC (Figure 1B). Although human cells of multiple immunophenotypes were present in most recipient mice, fractionation by magnetic beads-conjugated antibodies and subsequent real-time PCR analysis detected EBV DNA only in the predominant immunophenotypes that contained EBV DNA in the original patients (Figure 1B, Table 1). The EBV DNA load observed in individual lymphocyte subsets in the patient 3 and a mouse that received her PBMC is shown as supporting data (Table S1). When PBMC from three healthy EBV-carriers were injected intravenously to NOG mice, as controls, no EBV DNA was detected from either the peripheral blood, spleen, or liver (data not shown). Histological analyses of the spleen and the liver of these control mice identified no EBV-encoded small RNA (EBER)-positive cells, although some CD3-positive human T cells were observed (Figure S2). Analysis of TCR V $\beta$  repertoire demonstrated an identical predominant T-cell clone in patients (patients 1 and 3) and the corresponding mice that received their PBMC (Figure 1C). The general condition of most recipient mice deteriorated gradually in the observation period of eight to twelve weeks, with loss of body weight (Figure S1), ruffled hair, and inactivity.

NOG mice engrafted with EBV-infected T or NK cells were sacrificed for pathological and virological analyses between eight

**Table 1.** Patients with EBV-T/NK LPD and the results of xenotransplantation of their PBMC to NOG mice.

| Patient number | Diagnosis | Sex | Age | Type of infected cells | <sup>1</sup> EBV DNA load in the patients | <sup>2</sup> Engrafted cells in mice | <sup>3</sup> Engraftment | <sup>1</sup> EBV DNA load in mice |
|----------------|-----------|-----|-----|------------------------|---|--------------------------------------|--------------------------|-----------------------------------|
| 1              | CAEBV     | F   | 25  | CD4                    | 9.2×10 <sup>5</sup>                       | <u>CD4</u> , CD8                     | 3/3                      | 1.0~3.8×10 <sup>7</sup>           |
| 2              | CAEBV     | M   | 46  | CD4                    | 1.3~7.2×10 <sup>5</sup>                   | <u>CD4</u> , CD8                     | 2/2, 3/3                 | 2.6~10×10 <sup>5</sup>            |
| 3              | CAEBV     | F   | 35  | CD8                    | 2.1~78×10 <sup>5</sup>                    | <u>CD8</u> , CD4                     | 2/2, 2/2                 | 1.1~33×10 <sup>6</sup>            |
| 4              | CAEBV     | M   | 28  | CD8                    | 8.2×10 <sup>5</sup>                       | <u>CD8</u> , CD4                     | 3/3                      | 1.1~2.5×10 <sup>6</sup>           |
| 5              | CAEBV     | M   | 10  | γδT                    | 2.2×10 <sup>6</sup>                       | <u>γδT</u> , CD4, CD8                | 2/2                      | 3.8~6.5×10 <sup>6</sup>           |
| 6              | CAEBV     | F   | 15  | γδT                    | 6.2×10 <sup>5</sup>                       | <u>γδT</u> , CD4, CD8                | 2/2                      | 2.2~11×10 <sup>5</sup>            |
| 7              | CAEBV     | M   | 13  | NK                     | 1.1~6.7×10 <sup>5</sup>                   | <u>NK</u> , CD4, CD8                 | 2/2, 2/2                 | 0.6~15×10 <sup>4</sup>            |
| 8              | CAEBV     | F   | 13  | NK                     | 6.3×10 <sup>6</sup>                       | <u>NK</u> , CD4, CD8                 | 3/3, 2/2                 | 0.8~1.9×10 <sup>5</sup>           |
| 9              | CAEBV     | M   | 8   | NK                     | 1.2~8.7×10 <sup>5</sup>                   | <u>NK</u> , CD4, CD8                 | 2/2, 3/3                 | 1.8~7.2×10 <sup>5</sup>           |
| 10             | EBV-HLH   | M   | 10  | CD8                    | 2.8~38×10 <sup>4</sup>                    | <u>CD8</u> , CD4                     | 2/2, 2/2                 | 6.5~9.9×10 <sup>4</sup>           |
| 11             | EBV-HLH   | M   | 50  | CD8                    | 6.2×10 <sup>5</sup>                       | <u>CD8</u> , CD4                     | 4/4                      | 7.0~45×10 <sup>4</sup>            |
| 12             | EBV-HLH   | M   | 1   | CD8                    | 3.1×10 <sup>5</sup>                       | <u>CD8</u> , CD4                     | 2/2                      | 6.0~9.1×10 <sup>4</sup>           |
| 13             | EBV-HLH   | M   | 64  | CD8                    | 3.2~3.9×10 <sup>5</sup>                   | <u>CD8</u> , CD4                     | 2/2, 2/2                 | 5.0~30×10 <sup>5</sup>            |

<sup>1</sup>EBV DNA copies/μg DNA in the peripheral blood.

<sup>2</sup>EBV DNA was detected only in the cells of the underlined subsets.

<sup>3</sup>Number of mice with successful engraftment per number of recipient mice is shown for each experiment.

doi:10.1371/journal.ppat.1002326.t001

and twelve weeks post-transplantation. On autopsy, the majority of mice presented with splenomegaly, with slight hepatomegaly in occasional cases (Figure 2A). Histopathological findings obtained from a representative mouse (recipient of PBMC from the patient 3 (CD8 type)) are shown in Figure 2B and reveal infiltration of human CD3<sup>+</sup>CD20<sup>-</sup> cells to major organs, including the spleen, liver, lungs, kidneys, and small intestine. These cells were positive for both EBER and human CD45RO, indicating that they are EBV-infected human T cells (Figure 2B). In contrast, no EBV-infected T cells were found in mice transplanted with PBMC isolated from a normal EBV carrier (Figure S2). Histopathology of a control NOG mouse is shown in Figure S2. Morphologically, EBV-infected cells are relatively small and do not have marked atypia. The infiltration pattern was leukemic and identical with chronic active EBV infection in children [34]. The architecture of the organs was well preserved in spite of marked lymphoid infiltration. The spleen showed marked expansion of periarterial lymphatic sheath owing to lymphocytic infiltration. In the liver, a dense lymphocytic infiltration was observed in the portal area and in the sinusoid. The lung showed a picture of interstitial pneumonitis and the lymphocytes often formed nodular aggregations around bronchioles and arteries. In the kidney, dense lymphocytic infiltration caused interstitial nephritis. In the small intestine, mild lymphoid infiltration was seen in mucosa. Quantification of EBV DNA in the spleen, liver, lymph nodes, lungs, kidneys, adrenals, and small intestine of this mouse revealed EBV DNA at the levels of 1.5–5.1×10<sup>7</sup> copies/μg DNA. Mice transplanted with PBMC derived from CAEBV of other types exhibited similar infiltration of EBV-infected T or NK cells to the spleen, liver, and other organs (Figure 2C and data not shown).

**EBV-infected T- and NK-cell lines established from CAEBV patients do not engraft in NOG mice**

We established EBV-positive cell lines of CD4<sup>+</sup> T, CD8<sup>+</sup> T, γδT, and CD56<sup>+</sup> NK lineages from PBMC of the patients listed in Table 1 by the method described previously [35], and confirmed by flow cytometry that the surface phenotypes of EBV-infected cells in the original patients were retained in these cell lines (data

not shown). To test whether these cell lines engraft in NOG mice, 1–4×10<sup>6</sup> cells were injected intravenously to NOG mice. The results are shown in Figure 3A and indicate that CAEBV-derived cell lines of the CD8<sup>+</sup> T, γδT, and CD56<sup>+</sup> NK phenotypes do not engraft in NOG mice. Neither human CD45-positive cells nor EBV DNA were detected in the peripheral blood of the mice up to twelve weeks post-transplantation. When the recipient mice were sacrificed at twelve weeks post-injection, no EBV DNA could be detected in the spleen, liver, bone marrow, mesenteric lymph nodes, and kidneys. In contrast, the CD4<sup>+</sup> T cell lines derived from the CD4-type patients 1 and 2 engrafted in NOG mice and induced T lymphoproliferation similar to that induced by PBMC isolated freshly from these patients (Figure 3A and data not shown). These results, together with the results of transplantation with EBV-containing subsets of PBMC, indicate that EBV-infected T and NK cells, with the exception of those of the CD4<sup>+</sup> subset, are not able to engraft in NOG mice, when they are separated from other components of PBMC, suggesting that some components of PBMC are essential for the outgrowth EBV-infected T and NK cells in NOG mice.

**Engraftment of EBV-infected T and NK cells in NOG mice requires CD4<sup>+</sup> T cells**

To identify the cellular component required for the engraftment of EBV-infected T and NK cells in NOG mice, we transplanted PBMC of CAEBV patients after removing individual immunophenotypic subsets by magnetic beads-conjugated antibodies. The results are shown in Figure 3B and summarized in Table 2. With respect to the patients 3 and 4, in whom CD8<sup>+</sup> T cells are infected with EBV, removal of CD8<sup>+</sup> cells from PBMC, as expected, resulted in the failure of engraftment, whereas elimination of CD19<sup>+</sup>, CD56<sup>+</sup>, or CD14<sup>+</sup> cells did not affect engraftment. Importantly, elimination of CD4<sup>+</sup> cell fraction, that did not contain EBV DNA, resulted in the failure of engraftment of EBV-infected T cells (Figure 3B and data not shown). In the experiments with the patients 5 and 6, in whom γδT cells were infected, removal CD4<sup>+</sup> cells that did not contain EBV DNA, as well as that of γδT cells, resulted in the failure of engraftment.



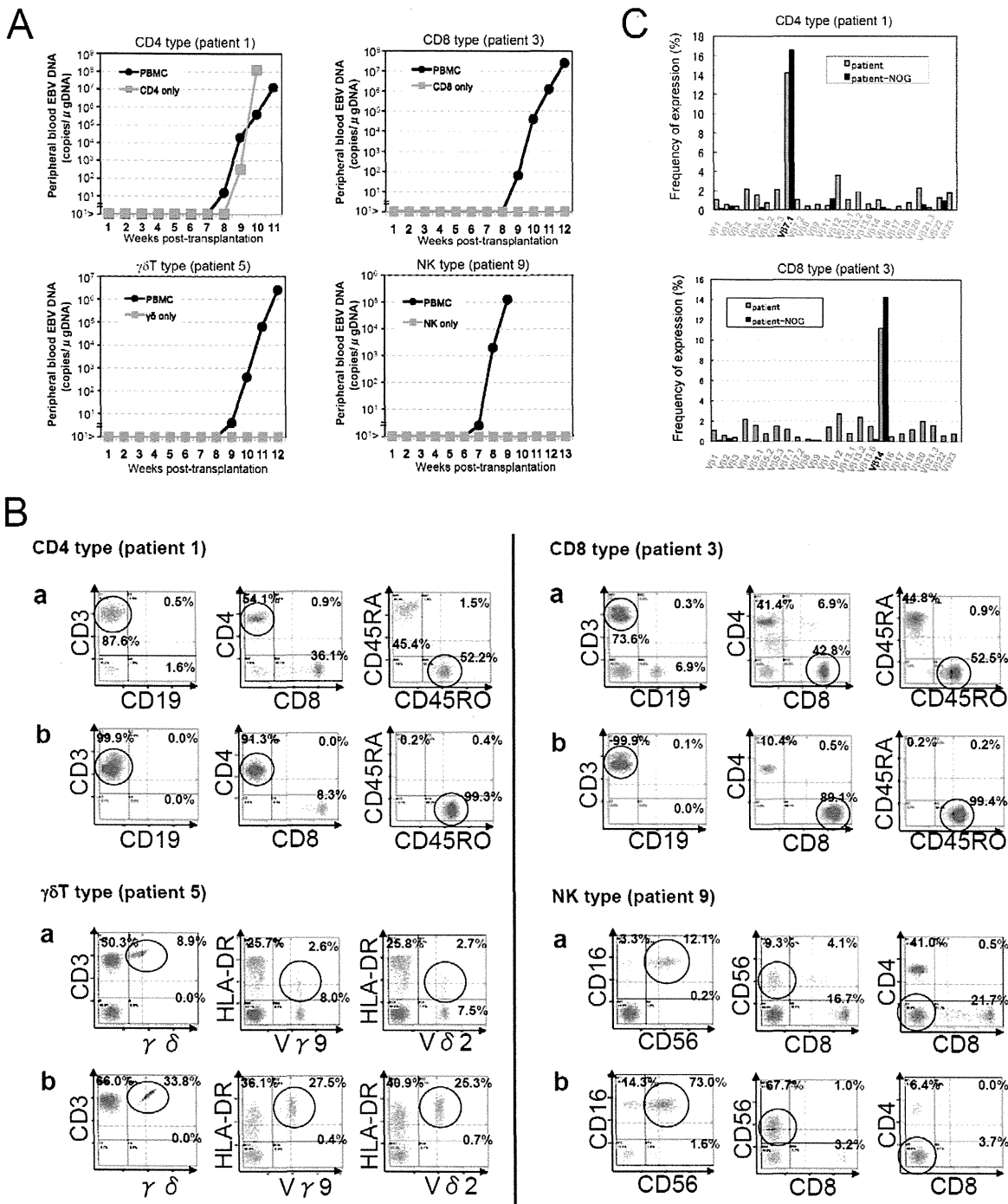


**Figure 1. Engraftment of EBV-infected T or NK cells in NOG mice following transplantation with PBMC of patients with CAEBV.** A. Measurement of EBV DNA levels. PBMC obtained from the CAEBV patients 1 (CD4 type), 3 (CD8 type), 5 ( $\gamma\delta$ T type), and 9 (NK type) were injected intravenously to NOG mice and EBV DNA load in their peripheral blood was measured weekly by real-time PCR. The results of transplantation with whole PBMC or with isolated EBV DNA-containing cell fraction are shown. B. Flow-cytometric analysis on the expression of surface markers in the peripheral blood lymphocytes of patients (a) with CAEBV and NOG mice (b) that received PBMC from them. Human lymphocytes gated by the pattern of side scatter and human CD45 expression were further analyzed for the expression of various surface markers indicated in the figures. The results from the patients 1, 3, 5, and 9, and the corresponding mice that received their respective PBMC are shown. Circles indicate the fractions that contained EBV DNA. C. Analysis on the expression of TCR V $\beta$  repertoire. Peripheral blood lymphocytes obtained from the patients 1 (CD4 type) and 3 (CD8 type), and from the corresponding mice that received their respective PBMC were analyzed for the expression of V $\beta$  alleles. The percentages of T cells expressing each V $\beta$  allele are shown for the patients (grey bars) and the mice (black bars). doi:10.1371/journal.ppat.1002326.g001

Removal of CD8<sup>+</sup>, CD14<sup>+</sup>, CD19<sup>+</sup>, or CD56<sup>+</sup> cells did not have an influence on the engraftment (Figure 3B and data not shown). Regarding the patients 8 and 9 in whom EBV resided in CD56<sup>+</sup>

NK cells, removal of CD4<sup>+</sup> as well as CD56<sup>+</sup> cells resulted in the failure of engraftment, whereas that of CD8<sup>+</sup>, CD19<sup>+</sup>, or CD14<sup>+</sup> cells did not affect engraftment (Figure 3B and data not shown). In

**Table 2.** Results of xenotransplantation with subsets of PBMC obtained from CAEBV patients.

| Number of patient | Diagnosis | Phenotype of infected cells | Cell fraction transplanted | Number of transplanted cells | Engraftment |
|-------------------|-----------|-----------------------------|----------------------------|------------------------------|-------------|
| 1                 | CAEBV     | CD4                         | PBMC                       | 2×10 <sup>6</sup>            | +           |
|                   |           |                             | CD4                        | 2×10 <sup>6</sup>            | +           |
|                   |           |                             | PBMC-CD4                   | 3×10 <sup>6</sup>            | –           |
|                   |           |                             | PBMC-CD8                   | 2×10 <sup>6</sup>            | +           |
|                   |           |                             | PBMC-CD56                  | 2×10 <sup>6</sup>            | +           |
|                   |           |                             | PBMC-CD14                  | 2×10 <sup>6</sup>            | +           |
|                   |           |                             | PBMC-CD19                  | 2×10 <sup>6</sup>            | +           |
| 3                 | CAEBV     | CD8                         | PBMC                       | 2×10 <sup>6</sup>            | +           |
|                   |           |                             | CD8                        | 3×10 <sup>6</sup>            | –           |
|                   |           |                             | PBMC-CD4                   | 3×10 <sup>6</sup>            | –           |
|                   |           |                             | PBMC-CD8                   | 3×10 <sup>6</sup>            | –           |
|                   |           |                             | PBMC-CD56                  | 2×10 <sup>6</sup>            | +           |
|                   |           |                             | PBMC-CD14                  | 2×10 <sup>6</sup>            | +           |
|                   |           |                             | PBMC-CD19                  | 2×10 <sup>6</sup>            | +           |
| 5                 | CAEBV     | γδT                         | PBMC                       | 2×10 <sup>6</sup>            | +           |
|                   |           |                             | γδT                        | 3×10 <sup>6</sup>            | –           |
|                   |           |                             | PBMC-CD4                   | 3×10 <sup>6</sup>            | –           |
|                   |           |                             | PBMC-γδT                   | 3×10 <sup>6</sup>            | –           |
|                   |           |                             | PBMC-CD8                   | 3×10 <sup>6</sup>            | +           |
|                   |           |                             | PBMC-CD56                  | 3×10 <sup>6</sup>            | +           |
|                   |           |                             | PBMC-CD14                  | 3×10 <sup>6</sup>            | +           |
| 9                 | CAEBV     | NK                          | PBMC                       | 2×10 <sup>6</sup>            | +           |
|                   |           |                             | NK                         | 3×10 <sup>6</sup>            | –           |
|                   |           |                             | PBMC-CD4                   | 3×10 <sup>6</sup>            | –           |
|                   |           |                             | PBMC-CD8                   | 3×10 <sup>6</sup>            | +           |
|                   |           |                             | PBMC-CD56                  | 3×10 <sup>6</sup>            | –           |
|                   |           |                             | PBMC-CD14                  | 3×10 <sup>6</sup>            | +           |
|                   |           |                             | PBMC-CD19                  | 3×10 <sup>6</sup>            | +           |
| 11                | EBV-HLH   | CD8                         | PBMC                       | 2×10 <sup>6</sup>            | +           |
|                   |           |                             | PBMC-CD4                   | 4×10 <sup>6</sup>            | –           |

doi:10.1371/journal.ppat.1002326.t002

the patients 1 and 2, in whom CD4<sup>+</sup> T cells were infected, only the removal of CD4<sup>+</sup> cells blocked the engraftment of EBV-infected cells and depletion of either CD8<sup>+</sup>, CD19<sup>+</sup>, or CD14<sup>+</sup> cells had no effect (Figure 3B and data not shown). These results suggested that EBV-infected cells of the CD8<sup>+</sup>, γδT, and CD56<sup>+</sup> lineages require CD4<sup>+</sup> cells for their engraftment in NOG mice. To confirm this interpretation, we performed complementation experiments, in which EBV-containing fractions of the CD8<sup>+</sup> (patient 4), γδT (patient 5), or CD56<sup>+</sup> (patient 7) phenotypes were transplanted together with autologous CD4<sup>+</sup> cells. The results are shown in Figure 3A and indicate that EBV-infected CD8<sup>+</sup>, γδT, or CD56<sup>+</sup> cells engraft in NOG mice when transplanted together with CD4<sup>+</sup> cells. Similarly, when EBV-infected cell lines of the CD8<sup>+</sup>, γδT, and CD16<sup>+</sup> lineages were injected intravenously to NOG mice together with autologous CD4<sup>+</sup> cells, these cell lines engrafted to the mice (Figure 3A). Finally, to further confirm the essential role of CD4<sup>+</sup> cells, we examined the effect of the OKT-4 antibody that depletes CD4<sup>+</sup> cells in vivo [24]. PBMC isolated from the CAEBV patient 3 (CD8 type) and the patient 8 (NK type) were injected

intravenously to NOG mice and OKT-4 was administered intravenously for four consecutive days starting from the day of transplantation. The results are shown in Figure 4 and indicate that OKT-4 can strongly suppress the engraftment of EBV-infected T and NK cells. In the mice treated with OKT-4, no splenomegaly was observed and EBV DNA was not detected either in the peripheral blood, spleen, liver, or lungs at eight weeks post-transplantation.

#### Analysis on the EBV gene expression associated with T or NK lymphoproliferation in NOG mice

Previous analysis of EBV gene expression in patients with CAEBV revealed the expression of EBNA1, LMP1, and LMP2A with the involvement of the Q promoter in the EBNA genes transcription and no expression of EBNA2, being consistent with the latency II type of EBV gene expression [36,37,38]. To test whether EBV-infected T and NK cells that proliferate in NOG mice retain this type of viral gene expression, we performed RT-PCR analysis in the spleen and the liver of mice that received

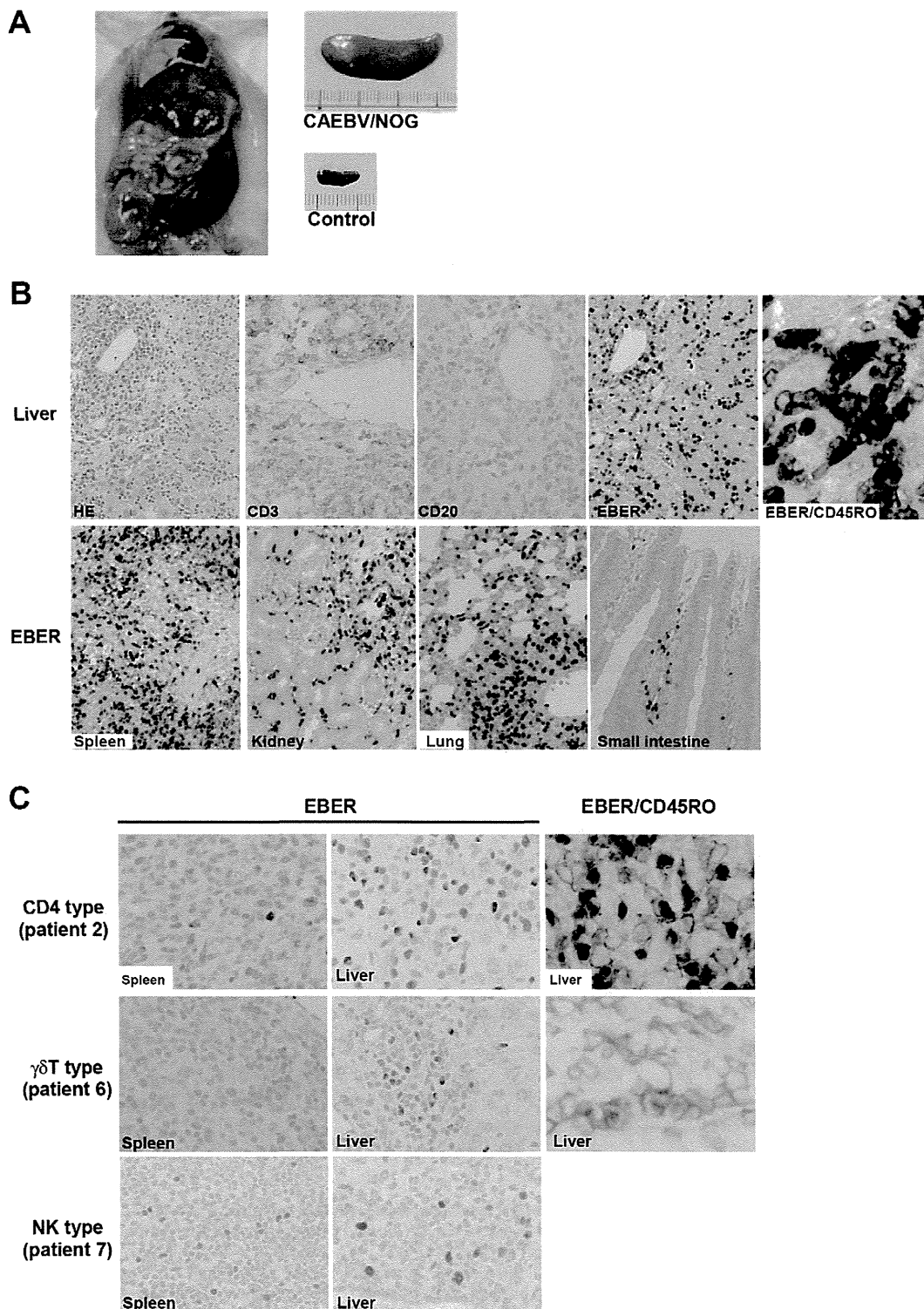


**Figure 2. Pathological and immunochemical analyses on NOG mice transplanted with PBMC from CAEBV patients.** A. Photographs of a model mouse showing splenomegaly and of the excised spleen. This mouse was transplanted with PBMC from the CAEBV patient 3 (CD8 type). Spleen from a control NOG mouse is also shown. B. Photomicrographs of various tissues of a mouse that received PBMC from the patient 3 (CD8 type). Upper panels: liver tissue was stained with hematoxylin-eosin (HE), antibodies specific to human CD3 or CD20, or by ISH with an EBER probe; the rightmost panel is a double staining with EBER and human CD45RO. Bottom panels: EBER ISH in the spleen, kidney, lung, and small intestine. Original magnification is  $\times 200$ , except for EBER/CD45RO, that is  $\times 400$ . C. Photomicrographs of the spleen and liver tissues obtained from NOG mice transplanted with PBMC from the CAEBV patients 2 (CD4 type), 6 ( $\gamma\delta$ T type) or 7 (NK type). Tissues were stained by EBER-ISH or by double staining with EBER-ISH and human CD45RO. Original magnification  $\times 600$ . doi:10.1371/journal.ppat.1002326.g002

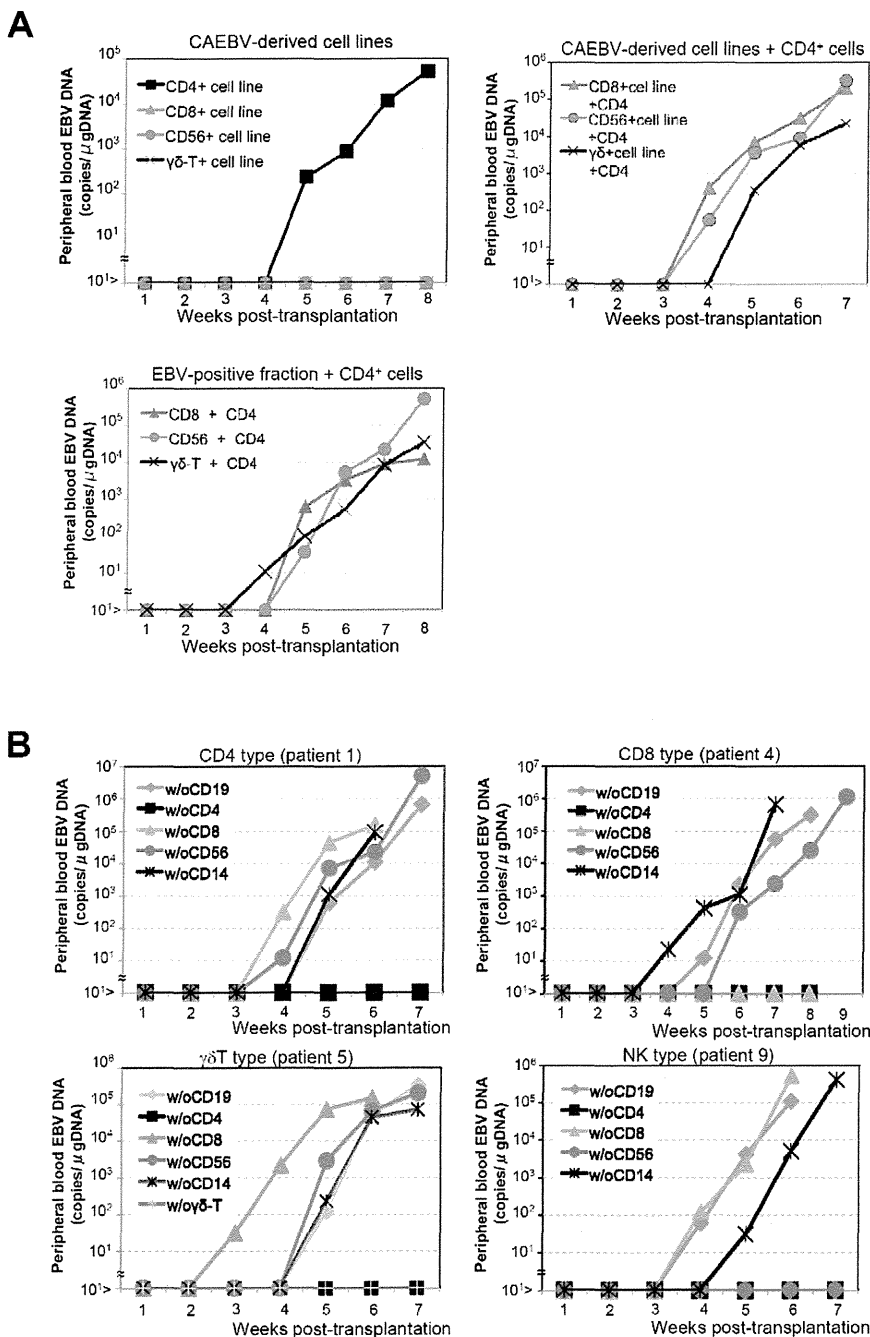


**Figure 3. Analysis on the conditions of the engraftment of EBV-infected T and NK cells in NOG mice.** A. EBV-infected T or NK cells isolated from patients with CAEBV or cell lines derived from them were injected to NOG mice in the conditions described below. Peripheral blood EBV DNA levels were then measured weekly. Upper-left panel:  $5 \times 10^6$  cells of EBV-infected CD4<sup>+</sup> T, CD8<sup>+</sup> T,  $\gamma\delta$ T, and CD56<sup>+</sup> NK cell lines established from the CAEBV patients 1, 4, 6, and 8, respectively, were injected intravenously to NOG mice. Upper-right panel:  $5 \times 10^6$  cells of the CD8<sup>+</sup> T,  $\gamma\delta$ T, and CD56<sup>+</sup> NK cell lines established from the patients 3, 6, and 8, respectively, were injected intravenously to NOG mice together with autologous CD4<sup>+</sup> T cells isolated from  $5 \times 10^6$  PBMC. Bottom panel:  $5 \times 10^6$  cells of the CD8<sup>+</sup> T,  $\gamma\delta$ T, and CD56<sup>+</sup> NK fractions isolated freshly from the patients 4, 5, and 7, respectively, were injected intravenously to NOG mice together with autologous CD4<sup>+</sup> T cells isolated from  $5 \times 10^6$  PBMC. B. Transplantation of PBMC devoid of individual immunophenotypic subsets to NOG mice. CD19<sup>+</sup>, CD4<sup>+</sup>, CD8<sup>+</sup>, CD56<sup>+</sup>, or CD14<sup>+</sup> cells were removed from PBMC obtained from the patient 1 (CD4 type, upper-left panel), 4 (CD8 type, upper-right), 5 ( $\gamma\delta$ T type, bottom-left), and 9 (NK type, bottom-right) and the remaining cells were injected intravenously to NOG mice. Thereafter peripheral blood EBV DNA was determined weekly. doi:10.1371/journal.ppat.1002326.g003

PBMC from the CAEBV patient 3 (CD8 type). The results are shown in Figure 5A and demonstrate the expression of mRNAs coding for EBNA1, LMP1, LMP2A, and LMP2B, but not for EBNA2. Expression of the EBV-encoded small RNA 1 (EBER1)

was also demonstrated. EBNA1 mRNAs transcribed from either the Cp promoter or the Wp promoter were not detected, whereas those transcribed from the Q promoter was abundantly detected. These results indicate that EBV-infected T cells retain the latency

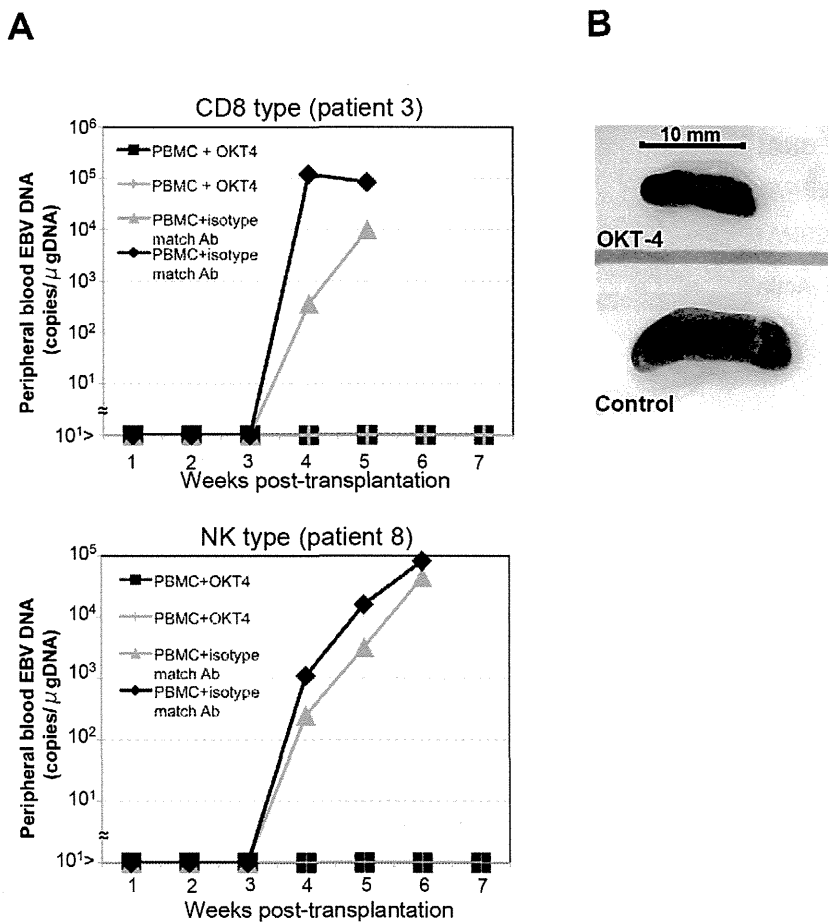


**Figure 4. Suppression of the engraftment of EBV-infected T and NK cells by the OKT-4 antibody.** PBMC ( $5 \times 10^6$  cells) isolated from the CAEBV patient 3 (CD8 type) or 8 (NK type) were injected intravenously to NOG mice. The OKT-4 antibody (100  $\mu\text{g}/\text{mouse}$ ) was administered intravenously on the same day of transplantation and the following three consecutive days. As a control, isotype-matched mouse IgG was injected. A. Changes in the peripheral blood EBV DNA level in the recipient mice. Results with the mice transplanted with PBMC of the patient 3 (top) and of the patient 8 (bottom) are shown. B. Photographs of the spleen of an OKT-4-treated mouse (top) and a control mouse (bottom) taken at autopsy. doi:10.1371/journal.ppat.1002326.g004

II pattern of latent EBV gene expression after engraftment in NOG mice. Similar analyses with NOG mice engrafted with EBV-infected NK cells also showed the latency II type of EBV gene expression (data not shown).

#### NOG mice engrafted with EBV-infected T or NK cells produce high levels of human cytokines

In patients with CAEBV, high levels of cytokines have been detected in the peripheral blood and are thought to play important roles in the pathogenesis [20,39,40]. To test whether this hypercytokinemia is reproduced in NOG mice, we examined the levels of various human cytokines in the sera of transplanted mice using ELISA kits that can quantify human cytokines specifically. The results are shown in Figure 5B and indicate that the mice transplanted with PBMC of the patient 3 (CD8 type) or the patient 8 (NK type) contained high levels of RANTES, IFN- $\gamma$ , and IL-8 in their sera.

#### Engraftment of EBV-infected T and B cells derived from patients with EBV-HLH in NOG mice

To extend the findings obtained from the CAEBV xenograft model to another disease with EBV<sup>+</sup> T/NK lymphoproliferation, we transplanted NOG mice with PBMC isolated from patients

with EBV-HLH. Characteristics of the four EBV-HLH patients examined in this study and the results of transplantation with their PBMC are summarized in Table 1. EBV DNA was detected in the peripheral blood three to four weeks post-transplantation and rapidly reached the levels of  $1 \times 10^4$  to  $1 \times 10^6$  copies/ $\mu\text{g}$  DNA (results of typical experiments are shown in Figure 6A). Similar to the findings in CAEBV, EBV DNA was not detected in the recipient mice, when CD4<sup>+</sup> cell fraction was removed from PBMC (Figure 6A). Immunophenotypic analyses on the peripheral blood lymphocytes isolated from EBV-HLH patients and corresponding recipient mice revealed that cells of an identical immunophenotype (CD3<sup>+</sup>CD8<sup>+</sup>CD45RO<sup>+</sup>CD19<sup>-</sup>CD4<sup>-</sup>CD45RA<sup>-</sup>CD16<sup>-</sup>CD56<sup>-</sup>) were present and contained EBV DNA in both the patients and corresponding mice (Figure 6C and data not shown). The EBV DNA load observed in individual lymphocyte subsets in the patient 10 and a mouse that received his PBMC is shown as supporting data (Table S2). General condition of the recipient mice deteriorated consistently more quickly, with the loss of body weight (Figure S1), ruffling of hair, and general inactivity, than those mice engrafted with EBV-infected T or NK cells derived from CAEBV. The mice were sacrificed around four weeks post-transplantation for pathological analyses. Macroscopical observation revealed moderate to severe splenomegaly (Figure 6D) in the

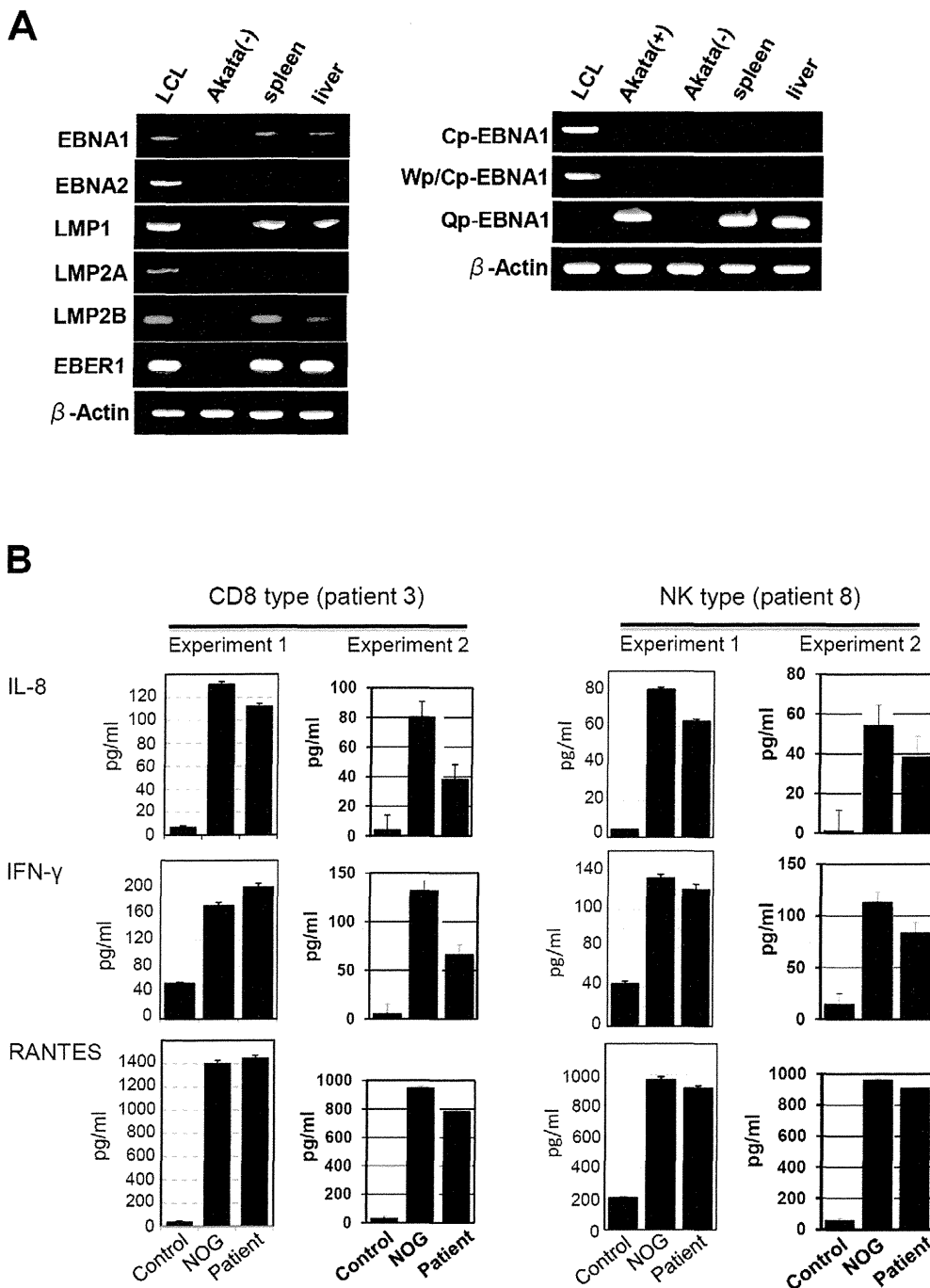


**Figure 5. Analyses on the latent EBV gene expression and cytokine production in NOG mice transplanted with PBMC of CAEBV patients.** A. EBV gene expression. Total RNA was purified from the spleen and liver of a mouse that received PBMC from the patient 3 (CD8 type) and applied for RT-PCR assay to detect transcripts from the indicated genes. RNA samples from an EBV-transformed B-lymphoblastoid cell line (LCL) and from EBV-negative Akata cell line were used as positive and negative controls, respectively. The primers used in the experiments are shown in Materials and Methods. B. Quantification of plasma levels of human cytokines in patients with CAEBV and corresponding recipient mice. PBMC were isolated from the patients 3 (CD8 type) and 8 (NK type) in two occasions and transplanted to NOG mice. Plasma cytokine levels of the patients were determined when their PBMC were isolated. Plasma cytokine levels of the corresponding recipient mice, prepared on each occasion of PBMC collection, were determined when they were sacrificed. Concentration of human IL-8, IFN- $\gamma$ , and RANTES were measured by appropriate ELISA kits following the instruction provided by the manufacturer. Plasma samples from healthy adults were used as a control. The bars represent mean values and standard errors from triplicate measurements. doi:10.1371/journal.ppat.1002326.g005

majority of recipient mice, and slight hepatomegaly in a limited fraction of them. A finding characteristic to these mice were massive hemorrhages in the abdominal and/or thoracic cavities,

that were not seen in the mice transplanted with CAEBV-derived PBMC (Figure 6D and data not shown). These hemorrhagic lesions may reflect coagulation abnormalities characteristic to

HLH. Histopathological analyses revealed a number of EBER<sup>+</sup> cells in the spleen and the liver (Figure 6E) and quantification of EBV DNA in these tissues revealed  $1.4 \times 10^1$  to  $2.4 \times 10^2$  copies/ $\mu$ g of EBV DNA. When the tissues were examined by immunostaining and EBER ISH, the EBER<sup>+</sup> cells were shown unexpectedly to be mostly CD45RO<sup>-</sup> and CD20<sup>+</sup> in all five transplantation experiments with four different patients, indicating that the majority of EBV-infected cells in these tissues are of the B-cell lineage (Figure 6E and data not shown). EBER<sup>+</sup> large B cells were seen scattered among numerous reactive small T cells, most of which are CD8<sup>+</sup>, in the tissues of the spleen, liver, lungs and kidneys. A number of macrophages were also seen in these tissues. Fractionation of mononuclear cells obtained from the liver of a mouse transplanted with PBMC of the EBV-HLH patient 10, followed by real-time PCR, detected EBV DNA ( $1.4 \times 10^1$  copies/ $\mu$ g DNA) only in the CD19<sup>+</sup> B-cell fraction. In addition, an EBV-infected B lymphoblastoid cell line, but not an EBV-positive T cell line, could be established from this liver. Thus the presence of EBV in B cells were demonstrated by three independent methods in the tissues of EBV-HLH mice. Enzyme-linked immunosorbent assay revealed extremely high levels of human cytokines, including IL-8, IFN- $\gamma$ , and RANTES, in the sera of both the original patients and the recipient mice (Figure 6B). The levels of IL-8 and IFN- $\gamma$  were much higher than those observed in the peripheral blood of patients with CAEBV and mice that received their PBMC. Thus, NOG mice transplanted with EBV-HLH-derived PBMC are distinct from those transplanted with CAEBV-derived PBMC in the aggressive time course of the disease, internal hemorrhagic lesions, extremely high levels of IL-8 and IFN- $\gamma$  in the peripheral blood, and the presence of EBV-infected B cells in lymphoid tissues.

## Discussion

The mouse xenograft models of CAEBV and EBV-HLH developed here represent the first recapitulation of EBV-associated T/NK lymphoproliferation in experimental animals. Previously, Hayashi and others inoculated rabbits with Herpesvirus papio and succeeded in the generation of T-cell lymphoproliferative disorder with pathological findings suggestive of EBV-HLH [41]. This model, however, is based on an EBV-related virus and not EBV itself, and therefore may contain features irrelevant to the original human disease. Although the CAEBV and EBV-HLH models described here exhibited some common features, including the abundant presence of EBV-infected T or NK cells in the peripheral blood, there were some critical differences between the two models, probably reflecting the divergence of the pathophysiology of the original diseases. First of all, in the EBV-HLH model mouse, EBV was detected mainly in B cells in the spleen and the liver, while it was found mainly in T cells in the peripheral blood. This makes an obvious contrast with the CAEBV model mouse, where EBV was detected in T or NK cells in both the peripheral blood and lymphoid tissues. We do not have an explanation for the apparent discrepancy in the host cell type of EBV infection between the peripheral blood and lymphoid tissues of the EBV-HLH model. It should be, however, noted that histopathology of EBV-HLH tissues has not been fully investigated and therefore it is still possible that significant number of EBV-infected B cells are present in the lymphoid tissues of EBV-HLH patients. Other differences between the two models include much higher plasma levels of IL-8 and IFN- $\gamma$  more aggressive and fatal outcome, and internal hemorrhagic lesions in EBV-HLH model mice, probably reflecting the differences in the pathophysiology of the original diseases.

EBV-positive B-cell proliferation was not seen in CAEBV model mice even in long-term observation beyond twelve weeks. This seems puzzling since low but significant amount of EBV DNA was found also in B19<sup>+</sup> B-cell fraction in most patients with CAEBV. It should be noted that EBV-infected T or NK cell lines could be established relatively easily from patients with CAEBV by adding recombinant IL-2 in the medium. In contrast, establishment of EBV-infected B LCLs from these patients has been extremely difficult. In fact, we could establish B-LCLs from a few patients with CAEBV only when their PBMC were cultured on feeder cells expressing CD40 ligand. Therefore, we speculate that in the particular context of CAEBV, both in the patient and the model mouse, proliferation of EBV-infected B cells are somehow inhibited by an unknown mechanism.

Analysis on the conditions of engraftment of EBV-infected T/NK cells using these new xenograft models revealed that EBV-infected T and NK cells of the CD8<sup>+</sup> T, TCR $\gamma$  $\delta$ T and CD56<sup>+</sup> NK lineages and cell lines derived from them require CD4<sup>+</sup> T cells for their engraftment in NOG mice. Only those EBV-infected cells and cell lines of the CD4<sup>+</sup> T lineage could engraft in NOG mice on their own. These findings suggest that some factor(s) provided by CD4<sup>+</sup> cells are essential for engraftment. Soluble factors produced by CD4<sup>+</sup> T cells may be responsible for this function and we are currently examining cytokines, including IL-2, for their ability to support the engraftment of EBV-infected T and NK cells. It is also possible that cell to cell contact involving CD4<sup>+</sup> cells is critical for engraftment. This dependence on CD4<sup>+</sup> cells represents an interesting consistency with the previous finding that engraftment of EBV-transformed B lymphoblastoid cells in *scid* mice required the presence of CD4<sup>+</sup> cells [42,43]. It has been speculated that T cells activated by an EBV-induced superantigen may be involved in the engraftment of EBV-infected B lymphoblastoid cells in *scid* mice [44]. Although a similar superantigen-mediated mechanism might also be assumed in T- and NK-cell lymphoproliferation in NOG mice, the data of TCR repertoire analyses (Figure 1C and data not shown) show no indication for clonal expansion of V $\beta$ 13 T cells that are known to be specifically activated by the EBV-induced superantigen HERV-K18. It seems therefore unlikely that this superantigen is involved in the CD4<sup>+</sup> T cell-dependent engraftment of EBV-infected T and NK cells. We expect CD4<sup>+</sup> T cells and/or molecules produced by them may be an excellent target in novel therapeutic strategies for the treatment of CAEBV and EBV-HLH. In fact, administration of the OKT-4 antibody that depletes CD4<sup>+</sup> cells *in vivo* efficiently prevented the engraftment of EBV-infected T cells. As a next step, we plan to test the effect of post-engraftment administration of OKT-4.

The dependence of EBV-infected T and NK cells on CD4<sup>+</sup> T cells for their engraftment in NOG mice suggests the possibility that these cells are not capable of autonomous proliferation. Consistent with this notion, EBV-infected T and NK cell lines, including that of the CD4<sup>+</sup> lineage, are dependent on IL-2 for their *in vitro* growth and do not engraft in either nude mice or *scid* mice when transplanted either *s.c.* or *i.v.* (Shimizu, N., unpublished results). Clinically, CAEBV is a disease of chronic time course and patients carrying monoclonal EBV-infected T or NK cell population may live for many years without progression of the disease [15]. Overt malignant T or NK lymphoma usually develops only after a long course of the disease. Taking all these findings in consideration, we suppose that EBV-infected cells are not truly malignant at least in the early phase of the disease, even when they appear monoclonal. Because infection of EBV in T or NK cells is not unique to CAEBV and has been recognized also in infectious mononucleosis [45,46], the critical deficiency in

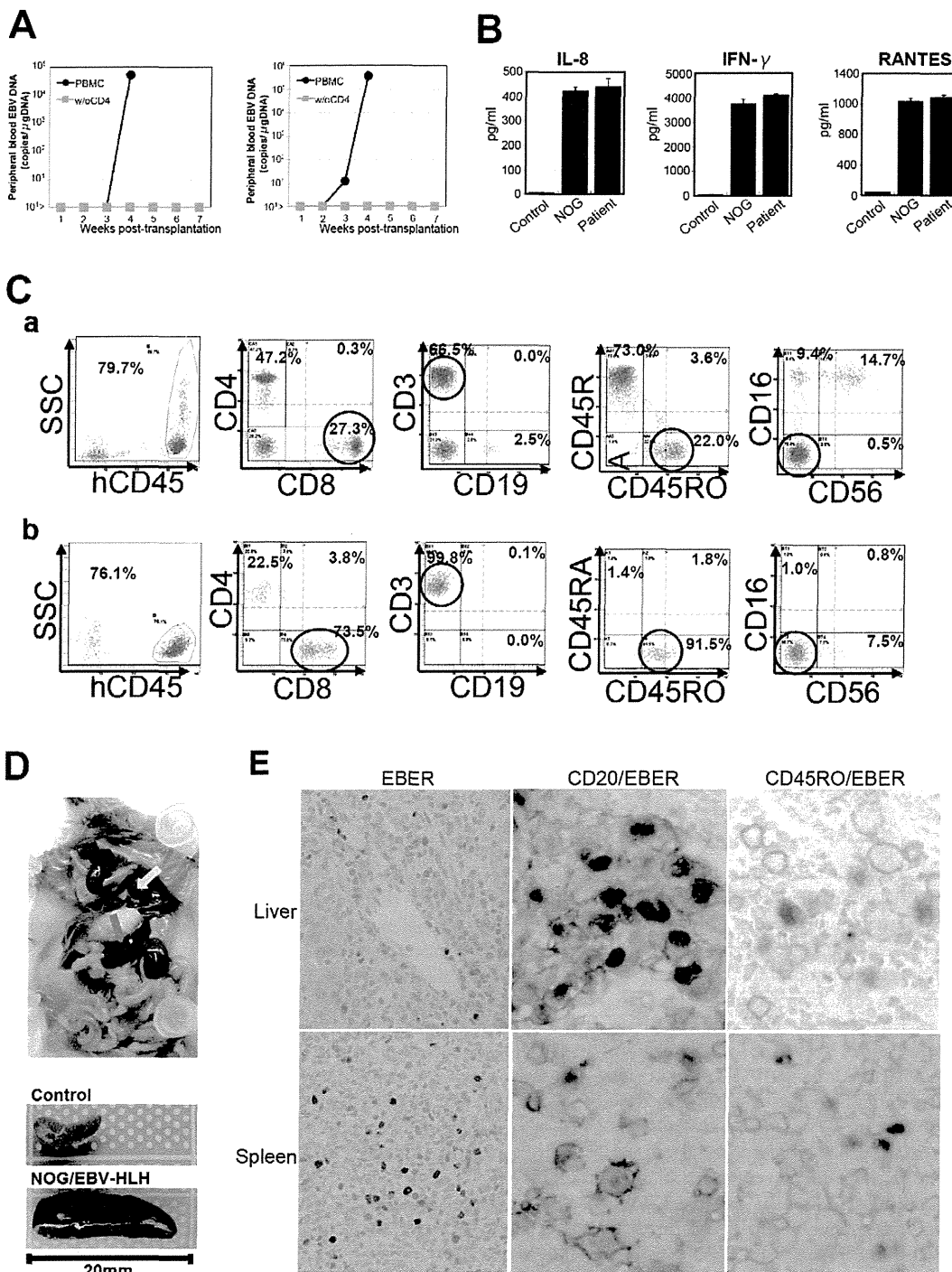


**Figure 6. Engraftment of EBV-infected T and B cells in NOG mice transplanted with PBMC of patients with EBV-HLH.** A. Peripheral blood EBV DNA load. Following transplantation with PBMC or PBMC devoid of CD4<sup>+</sup> cells of the patient 11, EBV DNA was measured weekly by real-time PCR. Results of two mice prepared in an experiment are shown. B. Cytokine levels in the peripheral blood of the patient 12 and a mouse that received his PBMC. The levels of IL-8, IFN- $\gamma$ , and RANTES were measured by ELISA in triplicates and the means and the standard errors are shown. A plasma sample of a healthy person was used as a control. C. Immunophenotypic analyses on the peripheral blood lymphocytes of the EBV-HLH patient 10 (a) and a mouse that received his PBMC (b). Lymphocytes were gated by the pattern of the side scatter and the expression of human CD45, and analyzed for the expression of the indicated markers. The circles indicate the fractions that contained EBV DNA. D. Photograph of a mouse showing splenomegaly (red arrow) and hemorrhagic lesions (yellow arrow). Spleens excised from this mouse and a control mouse are shown at the bottom. E. Photomicrographs of the tissues of mice transplanted with EBV-HLH-derived PBMC. Liver and spleen tissues of a mouse transplanted with PBMC of the patient 11 were examined by EBER-ISH (left), double staining with an anti-human CD20 monoclonal antibody and EBER-ISH (middle), and double staining with an anti-human CD45RO monoclonal antibody and EBER-ISH (right). Original magnification  $\times 600$ . doi:10.1371/journal.ppat.1002326.g006



CAEBV may be its inability to immunologically remove EBV-infected T and NK cells. In this context, it should be emphasized that EBV-infected T or NK cells usually exhibit the latency II pattern of EBV gene expression and do not express EBNA3s, that possess immuno-dominant epitopes recognized by EBV-specific T cells [47]. EBV-infected T and NK cells are thus not likely to be removed by cytotoxic T cells as efficiently as EBV-infected B cells that express EBNA3s. The reported lack of cytotoxic T cells specific to LMP2A [17], one of the few immuno-dominant EBV proteins expressed in the virus-infected T and NK cells, may therefore seriously affect the host's capacity to control their proliferation. A genetic defect in the perforin gene was recently identified in a patient with clinical and pathological features resembling CAEBV, suggesting that defects in genes involved in immune responses can result in clinical conditions similar to CAEBV [48].

Engraftment of EBV-infected T and NK cells in NOG mice was in most cases accompanied by co-engraftment of un-infected cell populations. These un-infected cells might have been maintained and induced to proliferate by certain factors produced by EBV-infected T or NK cells. Abundant cytokines produced by these cells may be responsible for this activity. It is also possible that the proliferation of these un-infected cells represents immune responses. Experiments are underway to test whether these un-infected T cells contain EBV-specific cells. These un-infected T cells might also be reacting to host murine tissues. Intravenous injection of PBMC obtained from normal humans to immunodeficient mice including NOG mice has been shown to induce acute or chronic graft versus host disease (GVHD) [49,50]. However, because much less PBMC were injected to mice in the present study as compared to those previous studies, it is not likely that major GVHD was induced in NOG mice transplanted with PBMC of patients with CAEBV or EBV-HLH.

CAEBV has been treated by a variety of regimens, including antiviral, cytotoxic, and immunomodulating agents with more or less unsatisfactory results. Although hematopoietic stem cell transplantation, especially that with reduced intensity conditioning can give complete remission in a substantial number of patients [51,52], it is still desirable to develop safer and more effective treatment, possibly with pharmaceutical agents. The xenograft model of CAEBV generated in this study may be an excellent animal model to test novel experimental therapies for the disease. In fact, the OKT-4 antibody that depletes CD4<sup>+</sup> T cells in vivo gave a promising result implying its effectiveness as a therapeutic to CAEBV.

## Materials and Methods

### Ethics statement

Protocols of the experiments with materials obtained from patients with CAEBV and EBV-HLH and from control persons have been reviewed and approved by the Institutional Review Boards of the National Center for Child Health and Development and of the National Institute of Infectious diseases (NIID). Blood samples of the patients and control persons were collected after obtaining written informed consent. Protocols of the experiments with NOG mice are in accordance with the Guidelines for Animal Experimentation of the Japanese Association for Laboratory Animal Science and were approved by the Institutional Animal Care and Use Committee of NIID.

### Patients with CAEBV and EBV-HLH

Characteristics of the nine patients with CAEBV and the four patients with EBV-HLH examined in this study are summarized

in Table 1. Diagnosis of CAEBV and EBV-HLH was made on the basis of the published guidelines [19,53] and confirmed by identification of EBV-infected T or NK cells in their peripheral blood by flow cytometry and real-time PCR.

### NOD/Shi-*scid*/IL2R $\gamma$ <sup>null</sup> (NOG) mice

Mice of the NOD/Shi-*scid*/IL-2R $\gamma$ <sup>null</sup> (NOG) strain [22] were obtained from the Central Institute for Experimental Animals (Kawasaki, Japan) and maintained under specific pathogen free (SPF) conditions in the animal facility of NIID, as described [22].

### Transplantation of PBMC or their subfractions to NOG mice

PBMC were isolated by centrifugation on Lymphosepar I (Immuno-Biological Laboratories (IBL)) and injected intravenously to the tail vein of NOG mice at the age of 6–8 weeks. Depending on the recovery of PBMC, 1–4 × 10<sup>6</sup> cells were injected to 2 to 4 mice in a typical experiment with a blood sample. For transplantation with individual cellular fractions containing EBV DNA, CD4<sup>+</sup> T cells, CD8<sup>+</sup> T cells, and CD56<sup>+</sup> NK cells were separated with the IMag Cell Separation Systems (BD Pharmingen) following the protocol supplied by the manufacturer. To isolate  $\gamma\delta$ T cells, CD19<sup>+</sup>, CD4<sup>+</sup>, CD8<sup>+</sup>, CD56<sup>+</sup>, and CD14<sup>+</sup> cells were serially removed from PBMC by the IMag Cell Separation Systems. From the remaining CD19<sup>-</sup>CD4<sup>-</sup>CD8<sup>-</sup>CD56<sup>-</sup>CD14<sup>-</sup> population, CD3<sup>+</sup> cells were positively selected by the same kit and defined as the  $\gamma\delta$ T cell fraction. To transplant PBMC lacking individual immunophenotypic subsets, CD19<sup>+</sup> CD4<sup>+</sup>, CD8<sup>+</sup>, CD56<sup>+</sup> or CD14<sup>+</sup> cells were removed from PBMC by the IMag Cell Separation Systems and the remaining cells were injected to mice. To prepare PBMC lacking  $\gamma\delta$ T cells, CD19<sup>+</sup>, CD4<sup>+</sup>, CD8<sup>+</sup>, CD56<sup>+</sup>, and CD14<sup>+</sup> cells isolated from PBMC in the process of obtaining  $\gamma\delta$ T cell fraction (see above) were pooled and mixed with the CD19<sup>-</sup>CD4<sup>-</sup>CD8<sup>-</sup>CD56<sup>-</sup>CD14<sup>-</sup> cells that did not react with anti-CD3 antibody. For complementation experiments, an EBV-containing cell fraction and the CD4<sup>+</sup> cell fraction were isolated from a sample of PBMC as described above and the mixture of these two fractions were injected to NOG mice. The approximate numbers of injected cells are shown in Table 2.

### Analysis of immunophenotypes and TCR repertoire expression by flow cytometry

PBMC isolated from the patients and the recipient NOG mice as described above were incubated for 30 min on ice with a mixture of appropriate combinations of fluorescently labeled monoclonal antibodies. After washing, five-color flow-cytometric analysis was carried out with the Cytomics FC500 analyzer (Beckman Coulter). The following directly labeled antibodies were used: phycoerythrin (PE)-conjugated antibodies to CD3, CD8, and TCR $\alpha/\beta$ , fluorescein isothiocyanate (FITC)-conjugated antibodies to CD3, CD4, CD8, CD19, TCRV $\gamma$ 9, TCRV $\delta$ 2, and TCR $\gamma/\delta$ , and Phycoerythrin Texas Red (ECD)-conjugated antibody to CD45RO from Beckman Coulter; PE-conjugated antibodies to CD16, CD40, and CD40L, and FITC-conjugated antibody to CD56 from BD Pharmingen. TCR V $\beta$  repertoire analysis was performed with the Multi-analysis TCR V $\beta$  antibodies Kit (Beckman Coulter) according to the procedure recommended by the manufacturer.

### Treatment of mice with the OKT-4 antibody

NOG mice were injected intravenously with 5 × 10<sup>6</sup> PBMC isolated from the CAEBV patient 3 (CD8 type) or 8 (NK type) and were subsequently injected intravenously with 100  $\mu$ g of the OKT-4 antibody on the same day of transplantation. Additional

administration of the antibody was carried out by the same dose and route for the following three consecutive days. Peripheral blood EBV DNA load was then monitored every week. Mice were finally sacrificed four weeks post-transplantation and applied for pathological and virological analyses.

**Quantification of EBV DNA by real time PCR and analysis of EBV gene expression by RT-PCR**

Quantification of EBV DNA was carried out by real-time quantitative PCR assay based on the TaqMan system (Applied Biosystems), as described [54]. Analysis of EBV gene expression by RT-PCR was carried out as previously described with the following primers [55]. EBNA1: sense, gatgagcgttgggagagctgattctgca; anti-sense, tcctcgtccatggttatcac. EBNA2: sense, agaggagtggtgaagcggttc; antisense, tgacgggttccaagactatcc. LMP1: sense, ctctccttctcctcttctg; antisense, caggagggtgatcatcatga. LMP2A: sense, atgactcatctcaacacata; antisense, catgttaggcaaatgcaaa. LMP2B: sense, cagtgtaatctgcacaaaga; antisense, catgttaggcaaatgcaaa. EBER1: sense, agcacc-tacgctgcctaga; antisense, aaacatcgccgaccaccagc. Cp-EBNA1: sense, cactacaagacctagcctctccattcat; anti sense, ttcggtctcccttagccctcg. Wp/Cp-EBNA1: sense, tcagagcgccaggagtcacacaaaat; anti-sense, ttcggtctcccttagccctcg. Qp-EBNA1: sense, aggcgcgggagtagcgtgcctaccgga; antisense, tcctcgtccatggttatcac. RT-PCR primers for  $\beta$ -actin were purchased from Takara (Osaka, Japan).

**Histopathology, EBER ISH, and immunohistochemistry**

Tissue samples were fixed in 10% buffered formalin, embedded in paraffin, and stained with hematoxylin and eosin. For phenotypic analysis of engrafted lymphocytes, immunostaining for CD3, CD8 (Nichirei), CD45RO, and CD20 (DAKO) was performed on paraffin sections. EBV was detected by in situ hybridization (ISH) with EBV small RNA (EBER) probe. Immunohistochemistry and ISH were performed on an automated stainer (BENCHMARK XT, Ventana Medical Systems) according to the manufacturer’s recommendations. To determine the cell lineage of EBV infected cells, paraffin sections were applied to double staining with EBER ISH and immunohistochemistry. Immediately following EBER ISH, immunostaining for CD45RO or CD20 was performed. Photomicrographs was acquired with a OLYMPUS BX51 microscope equipped with 40x/0.75 and 20x/0.50 Uplan Fl objective lens, a Pixera Penguin 600CL digital camera (Pixera), and Viewfinder 3.01 (Pixera) for white balance, contrast, and brightness correction.

**Quantification of cytokines**

The levels of human IL-8, IFN- $\gamma$ , and RANTES in plasma samples were measured with the Enzyme-linked immunosorbent assay (ELISA) kit provided by R&D Systems following instructions provided by the manufacturer.

**References**

1. Rickinson AB, Kieff ED (2007) Epstein-Barr virus. In: Knipe DM, Howley PM, eds. *Fields Virology* 5. ed. Philadelphia: Lippincott Williams and Wilkins. pp 2655–2700.
2. Kieff ED, Rickinson AB (2007) Epstein-Barr virus and its replication. In: Knipe DM, Howley PM, eds. *Fields Virology*. Philadelphia: Lippincott Williams and Wilkins. pp 2603–2654.
3. Fujiwara S, Ono Y (1995) Isolation of Epstein-Barr virus-infected clones of the human T-cell line MT-2: use of recombinant viruses with a positive selection marker. *J Virol* 69: 3900–3903.
4. Watry D, Hedrick JA, Siervo S, Rhodes G, Lamberti JJ, et al. (1991) Infection of human thymocytes by Epstein-Barr virus. *J Exp Med* 173: 971–980.

**Accession numbers**

The Swiss-Prot accession numbers for the proteins described in this article are as follows: P13501 for RANTES; P10145 for IL-8; P01579 for IFN- $\gamma$ ; P03211 for EBNA1; P12978 for EBNA2; P12977 for EBNA3; P03230 for LMP1; and Q66562 for LMP2. The DDBJ accession number for EBER is AJ315772.

**Supporting Information**

**Figure S1** Changes in the body weight of NOG mice transplanted with PBMC derived from patients with CAEBV or EBV-HLH. Body weight of the five CAEBV mice shown in Figure 1A (transplanted with PBMC from the patient 1, 3, 5, and 9, and with the CD4<sup>+</sup> fraction from the patient 1, respectively) and two EBV-HLH mice shown in Figure 6A (both transplanted with PBMC from the patient 11) were recorded weekly. (TIF)

**Figure S2** Histopathological analysis of a control NOG mouse. A. a NOG mouse without xenograft. A 20-week old female NOG mouse was sacrificed and examined as a reference. No human cells are identified in these tissues. Upper panels: liver tissue was stained with hematoxylin-eosin (HE), antibodies specific to human CD3 or CD20, or by ISH with an EBER probe; the rightmost panel is a double staining with EBER and human CD45RO. Bottom panels: EBER ISH in the spleen, kidney, and small intestine. B. a NOG mouse transplanted with PBMC of a healthy EBV carrier. A six-week old female NOG mouse was transplanted with  $5 \times 10^6$  PBMC isolated from a normal EBV-seropositive person and sacrificed at eight weeks post-transplantation for histological analysis. Liver and Spleen tissues were stained with HE, antibodies specific to human CD3 or CD20, or by ISH with an EBER probe. No EBER-positive cells were identified in these tissues. Original magnification is  $\times 200$  for both A and B. (TIF)

**Table S1** EBV DNA load in lymphocyte subsets of a patient with CAEBV and a corresponding mouse derived from her PBMC. (DOC)

**Table S2** EBV DNA load in lymphocyte subsets of a patient with EBV-HLH and a corresponding mouse derived from his PBMC. (DOC)

**Acknowledgments**

We thank Kumiko Tanaka, Ken Watanabe, and Miki Katayama for technical assistance.

**Author Contributions**

Conceived and designed the experiments: KI MY NS NY SF. Performed the experiments: KI MY AN FK SI HN. Analyzed the data: KI MY AN SF. Contributed reagents/materials/analysis tools: AA TM SO MI OM JK. Wrote the paper: KI SF.

9. Kikuta H, Taguchi Y, Tomizawa K, Kojima K, Kawamura N, et al. (1988) Epstein-Barr virus genome-positive T lymphocytes in a boy with chronic active EBV infection associated with Kawasaki-like disease. *Nature* 333: 455–457.
10. Ishihara S, Tawa A, Yumura-Yagi K, Murata M, Hara J, et al. (1989) Clonal T-cell lymphoproliferation containing Epstein-Barr (EB) virus DNA in a patient with chronic active EB virus infection. *Jpn J Cancer Res* 80: 99–101.
11. Jaffe ES (2009) The 2008 WHO classification of lymphomas: implications for clinical practice and translational research. *Hematology Am Soc Hematol Educ Program* 2009: 523–531.
12. Okano M (2002) Overview and problematic standpoints of severe chronic active Epstein-Barr virus infection syndrome. *Crit Rev Oncol Hematol* 44: 273–282.
13. Straus SE (1992) Acute progressive Epstein-Barr virus infections. *Annu Rev Med* 43: 437–449.
14. Kimura H (2006) Pathogenesis of chronic active Epstein-Barr virus infection: is this an infectious disease, lymphoproliferative disorder, or immunodeficiency? *Rev Med Virol* 16: 251–261.
15. Kimura H, Morishima T, Kanegane H, Ohga S, Hoshino Y, et al. (2003) Prognostic factors for chronic active Epstein-Barr virus infection. *J Infect Dis* 187: 527–533.
16. Tsuge I, Morishima T, Kimura H, Kuzushima K, Matsuoka H (2001) Impaired cytotoxic T lymphocyte response to Epstein-Barr virus-infected NK cells in patients with severe chronic active EBV infection. *J Med Virol* 64: 141–148.
17. Sugaya N, Kimura H, Hara S, Hoshino Y, Kojima S, et al. (2004) Quantitative analysis of Epstein-Barr virus (EBV)-specific CD8+ T cells in patients with chronic active EBV infection. *J Infect Dis* 190: 985–988.
18. Aoukaty A, Lee IF, Wu J, Tan R (2003) Chronic active Epstein-Barr virus infection associated with low expression of leukocyte-associated immunoglobulin-like receptor-1 (LAIR-1) on natural killer cells. *J Clin Immunol* 23: 141–145.
19. Henter JI, Horne A, Arico M, Egeler RM, Filipovich AH, et al. (2007) HLH-2004: Diagnostic and therapeutic guidelines for hemophagocytic lymphohistiocytosis. *Pediatr Blood Cancer* 48: 124–131.
20. Lay JD, Tsao CJ, Chen JY, Kadin ME, Su IJ (1997) Upregulation of tumor necrosis factor- $\alpha$  gene by Epstein-Barr virus and activation of macrophages in Epstein-Barr virus-infected T cells in the pathogenesis of hemophagocytic syndrome. *J Clin Invest* 100: 1969–1979.
21. Imashuku S, Hibi S, Ohara T, Iwai A, Sako M, et al. (1999) Effective control of Epstein-Barr virus-related hemophagocytic lymphohistiocytosis with immunotherapy. *Histiocyte Society. Blood* 93: 1869–1874.
22. Ito M, Hiramatsu H, Kobayashi K, Suzue K, Kawahata M, et al. (2002) NOD/SCID/ $\gamma$ (c)(null) mouse: an excellent recipient mouse model for engraftment of human cells. *Blood* 100: 3175–3182.
23. Shultz LD, Lyons BL, Burzenski LM, Gott B, Chen X, et al. (2005) Human lymphoid and myeloid cell development in NOD/LtSz-scid IL2R  $\gamma$  null mice engrafted with mobilized human hemopoietic stem cells. *J Immunol* 174: 6477–6489.
24. Strowig T, Gurer C, Floss A, Liu YF, Arrey F, et al. (2009) Priming of protective T cell responses against virus-induced tumors in mice with human immune system components. *J Exp Med* 206: 1423–1434.
25. Watanabe S, Terashima K, Ohta S, Horibata S, Yajima M, et al. (2007) Hematopoietic stem cell-engrafted NOD/SCID/IL2R $\gamma$  null mice develop human lymphoid systems and induce long-lasting HIV-1 infection with specific humoral immune responses. *Blood* 109: 212–218.
26. Yajima M, Imadome K, Nakagawa A, Watanabe S, Terashima K, et al. (2008) A new humanized mouse model of Epstein-Barr virus infection that reproduces persistent infection, lymphoproliferative disorder, and cell-mediated and humoral immune responses. *J Infect Dis* 198: 673–682.
27. Traggiai E, Chicha L, Mazzucchelli L, Bronz L, Piffaretti JC, et al. (2004) Development of a human adaptive immune system in cord blood cell-transplanted mice. *Science* 304: 104–107.
28. Melkus MW, Estes JD, Padgett-Thomas A, Gatlin J, Denton PW, et al. (2006) Humanized mice mount specific adaptive and innate immune responses to EBV and TSST-1. *Nat Med* 12: 1316–1322.
29. Baenziger S, Tussiwand R, Schlaepfer E, Mazzucchelli L, Heikenwalder M, et al. (2006) Disseminated and sustained HIV infection in CD34+ cord blood cell-transplanted Rag2-/ $\gamma$  c-/- mice. *Proc Natl Acad Sci U S A* 103: 15951–15956.
30. Zhang L, Kovalev GI, Su L (2007) HIV-1 infection and pathogenesis in a novel humanized mouse model. *Blood* 109: 2978–2981.
31. Dewan MZ, Watanabe M, Ahmed S, Terashima K, Horiuchi S, et al. (2005) Hodgkin's lymphoma cells are efficiently engrafted and tumor marker CD30 is expressed with constitutive nuclear factor- $\kappa$ B activity in unconditioned NOD/SCID/ $\gamma$ mac(null) mice. *Cancer Sci* 96: 466–473.
32. Ishikawa F, Yoshida S, Saito Y, Hijikata A, Kitamura H, et al. (2007) Chemotherapy-resistant human AML stem cells home to and engraft within the bone-marrow endosteal region. *Nat Biotechnol* 25: 1315–1321.
33. Durig J, Ebeling P, Grabellus F, Sorg UR, Mollmann M, et al. (2007) A novel nonobese diabetic/severe combined immunodeficient xenograft model for chronic lymphocytic leukemia reflects important clinical characteristics of the disease. *Cancer Res* 67: 8653–8661.
34. Nakagawa A, Ito M, Saga S (2002) Fatal cytotoxic T-cell proliferation in chronic active Epstein-Barr virus infection in childhood. *Am J Clin Pathol* 117: 283–290.
35. Nagata H, Konno A, Kimura N, Zhang Y, Kimura M, et al. (2001) Characterization of novel natural killer (NK)-cell and gammadelta T-cell lines established from primary lesions of nasal T/NK-cell lymphomas associated with the Epstein-Barr virus. *Blood* 97: 708–713.
36. Imai S, Sugiura M, Oikawa O, Koizumi S, Hirao M, et al. (1996) Epstein-Barr virus (EBV)-carrying and -expressing T-cell lines established from severe chronic active EBV infection. *Blood* 87: 1446–1457.
37. Yoshioka M, Ishiguro N, Ishiko H, Ma X, Kikuta H, et al. (2001) Heterogeneous, restricted patterns of Epstein-Barr virus (EBV) latent gene expression in patients with chronic active EBV infection. *J Gen Virol* 82: 2385–2392.
38. Kimura H, Hoshino Y, Hara S, Sugaya N, Kawada J, et al. (2005) Differences between T-cell type and natural killer cell-type chronic active Epstein-Barr virus infection. *J Infect Dis* 191: 531–539.
39. Xu J, Ahmad A, Jones JF, Dolcetti R, Vaccher E, et al. (2000) Elevated serum transforming growth factor beta1 levels in Epstein-Barr virus-associated diseases and their correlation with virus-specific immunoglobulin A (IgA) and IgM. *J Virol* 74: 2443–2446.
40. Ohga S, Nomura A, Takada H, Ihara K, Kawakami K, et al. (2001) Epstein-Barr virus (EBV) load and cytokine gene expression in activated T cells of chronic active EBV infection. *J Infect Dis* 183: 1–7.
41. Hayashi K, Ohara N, Teramoto N, Onoda S, Chen HL, et al. (2001) An animal model for human EBV-associated hemophagocytic syndrome: herpesvirus papio frequently induces fatal lymphoproliferative disorders with hemophagocytic syndrome in rabbits. *Am J Pathol* 158: 1533–1542.
42. Veronese ML, Veronesi A, D'Andrea E, Del Mistro A, Indraco S, et al. (1992) Lymphoproliferative disease in human peripheral blood mononuclear cell-injected SCID mice. I. T lymphocyte requirement for B cell tumor generation. *J Exp Med* 176: 1763–1767.
43. Johannessen I, Asghar M, Crawford DH (2000) Essential role for T cells in human B-cell lymphoproliferative disease development in severe combined immunodeficient mice. *Br J Haematol* 109: 600–610.
44. Sutkowski N, Palkama T, Ciurli C, Sekaly RP, Thorley-Lawson DA, et al. (1996) An Epstein-Barr virus-associated superantigen. *J Exp Med* 184: 971–980.
45. Anagnostopoulos I, Hummel M, Kreschel C, Stein H (1995) Morphology, immunophenotype, and distribution of latently and/or productively Epstein-Barr virus-infected cells in acute infectious mononucleosis: implications for the interindividual infection route of Epstein-Barr virus. *Blood* 85: 744–750.
46. Hudnall SD, Ge Y, Wei L, Yang NP, Wang HQ, et al. (2005) Distribution and phenotype of Epstein-Barr virus-infected cells in human pharyngeal tonsils. *Mod Pathol* 18: 519–527.
47. Hislop AD, Taylor GS, Sauce D, Rickinson AB (2007) Cellular responses to viral infection in humans: lessons from Epstein-Barr virus. *Annu Rev Immunol* 25: 587–617.
48. Katano H, Ali MA, Patera AC, Catalano M, Jaffe ES, et al. (2004) Chronic active Epstein-Barr virus infection associated with mutations in perforin that impair its maturation. *Blood* 103: 1244–1252.
49. van Rijn RS, Simonetti ER, Hagenbeek A, Hogenes MC, de Weger RA, et al. (2003) A new xenograft model for graft-versus-host disease by intravenous transfer of human peripheral blood mononuclear cells in RAG2-/ $\gamma$  double-mutant mice. *Blood* 102: 2522–2531.
50. Ito R, Katano I, Kawai K, Hirata H, Ogura T, et al. (2009) Highly sensitive model for xenogenic GVHD using severe immunodeficient NOG mice. *Transplantation* 87: 1654–1658.
51. Kawa K, Sawada A, Sato M, Okamura T, Sakata N, et al. (2011) Excellent outcome of allogeneic hematopoietic SCT with reduced-intensity conditioning for the treatment of chronic active EBV infection. *Bone Marrow Transplant* 46: 77–83.
52. Sato E, Ohga S, Kuroda H, Yoshida F, Nishimura M, et al. (2008) Allogeneic hematopoietic stem cell transplantation for Epstein-Barr virus-associated T/natural killer-cell lymphoproliferative disease in Japan. *Am J Hematol* 83: 721–727.
53. Okano M, Kawa K, Kimura H, Yachie A, Wakiguchi H, et al. (2005) Proposed guidelines for diagnosing chronic active Epstein-Barr virus infection. *Am J Hematol* 80: 64–69.
54. Kimura H, Morita M, Yabuta Y, Kuzushima K, Kato K, et al. (1999) Quantitative analysis of Epstein-Barr virus load by using a real-time PCR assay. *J Clin Microbiol* 37: 132–136.
55. Nakamura H, Iwakiri D, Ono Y, Fujiwara S (1998) Epstein-Barr-virus-infected human T-cell line with a unique pattern of viral-gene expression. *Int J Cancer* 76: 587–594.

# Epstein-Barr Virus Induces Erosive Arthritis in Humanized Mice

Yoshikazu Kuwana<sup>1</sup>, Masami Takei<sup>1\*</sup>, Misako Yajima<sup>2</sup>, Ken-Ichi Imadome<sup>3</sup>, Hirotake Inomata<sup>1</sup>, Masaaki Shiozaki<sup>1</sup>, Natsumi Ikumi<sup>1</sup>, Takamasa Nozaki<sup>1</sup>, Hidetaka Shiraiwa<sup>1</sup>, Noboru Kitamura<sup>1</sup>, Jin Takeuchi<sup>1</sup>, Shigemasa Sawada<sup>1</sup>, Naoki Yamamoto<sup>2</sup>, Norio Shimizu<sup>4</sup>, Mamoru Ito<sup>5</sup>, Shigeyoshi Fujiwara<sup>3\*</sup>

**1** Division of Hematology and Rheumatology, Department of Medicine, Nihon University School of Medicine, Tokyo, Japan, **2** Department of Microbiology, Yong Loo Lin School of Medicine, National University of Singapore, Singapore, **3** Department of Infectious Diseases, National Research Institute for Child Health and Development, Tokyo, Japan, **4** Department of Virology, Division of Medical Science, Medical Research Institute, Tokyo Medical and Dental University, Tokyo, Japan, **5** Central Institute for Experimental Animals, Kawasaki, Japan

## Abstract

Epstein-Barr virus (EBV) has been implicated in the pathogenesis of rheumatoid arthritis (RA) on the basis of indirect evidence, such as its presence in affected joint tissues, antigenic cross reactions between EBV and human proteins, and elevated humoral and cellular anti-EBV immune responses in patients. Here we report development of erosive arthritis closely resembling RA in humanized mice inoculated with EBV. Human immune system components were reconstituted in mice of the NOD/Shi-*scid*/IL-2R $\gamma^{\text{null}}$  (NOG) strain by transplantation with CD34<sup>+</sup> hematopoietic stem cells isolated from cord blood. These humanized mice were then inoculated with EBV and examined pathologically for the signs of arthritis. Erosive arthritis accompanied by synovial membrane proliferation, pannus formation, and bone marrow edema developed in fifteen of twenty-three NOG mice transplanted with human HSC and inoculated with EBV, but not in the nine NOG mice that were transplanted with HSC but not inoculated with EBV. This is the first report of an animal model of EBV-induced arthritis and strongly suggest a causative role of the virus in RA.

**Citation:** Kuwana Y, Takei M, Yajima M, Imadome K-I, Inomata H, et al. (2011) Epstein-Barr Virus Induces Erosive Arthritis in Humanized Mice. PLoS ONE 6(10): e26630. doi:10.1371/journal.pone.0026630

**Editor:** Matthias G. von Herrath, La Jolla Institute of Allergy and Immunology, United States of America

**Received:** August 26, 2011; **Accepted:** September 29, 2011; **Published:** October 19, 2011

**Copyright:** © 2011 Takei et al. This is an open-access article distributed under the terms of the Creative Commons Attribution License, which permits unrestricted use, distribution, and reproduction in any medium, provided the original author and source are credited.

**Funding:** This study was supported by grants from the Ministry of Health, Labour and Welfare of Japan (H22-Nanchi-080 and H22-AIDS-002: <http://www.mhlw.go.jp/>), the Grant of National Center for Child Health and Development (22A-9: <http://www.ncchd.go.jp/>), and Strategic Research Base Development; Program for Private Universities subsidized by MEXT (S0801033 2010: [http://www.mext.go.jp/a\\_menu/koutou/shinkou/07021403/002/002/1218299.htm](http://www.mext.go.jp/a_menu/koutou/shinkou/07021403/002/002/1218299.htm)). The funders had no role in study design, data collection and analysis, decision to publish, or preparation of the manuscript.

**Competing Interests:** The authors have declared that no competing interests exist.

\* E-mail: takei.masami@nihon-u.ac.jp (MT); shige@nch.go.jp (SF)

© These authors contributed equally to this work.

## Introduction

A number of observations including those by the authors have suggested the involvement of Epstein-Barr virus (EBV) in the pathogenesis of rheumatoid arthritis (RA) [1,2,3,4,5,6,7]. For example, circulating EBV load is higher in RA patients than in healthy controls [8] and activated CD8-positive cells specific to EBV are commonly seen in RA patients [9]. Further, studies have reported that a large number of T cells specific to EBV-encoded proteins are present in the affected joints of RA patients [10], that interference of suppressor T cells specific to EBV plays a role in RA [11], and that RA patients have abnormally large numbers of EBV-infected B cells in the blood [12]. We have reported on the decreased expression of the gene coding for the signaling lymphocytic activation molecule-associated protein (SAP) (also known as the Src homology 2 domain-containing protein 1A (SH2D1A)) that is supposed to have critical roles in the elimination of EBV-infected B cells by cytotoxic T cells and NK cells [13]. This reduced expression of SAP might lead to the failure of the immune system to eliminate EBV-infected B cells in RA patients [14]. These studies, however, provided only indirect evidence for the involvement of EBV in RA and there have been

no published reports on EBV-induced arthritis in experimental animals.

Although model animals for EBV infection are required to examine a causal relationship between EBV and RA, there has been no appropriate animal models suitable for this purpose. EBV can infect only limited primate species and does not infect normal mice. Recently, we developed a humanized mouse model of EBV infection, based on the NOD/Shi-*scid*/IL-2R $\gamma^{\text{null}}$  (NOG) mouse strain [15], that can reproduce key aspects of human EBV infection, such as lymphoproliferative disorder, asymptomatic persistent infection, and humoral and T cell-mediated immune responses [15]. In this model, where human immune components were reconstituted by transplantation with cord blood-derived CD34<sup>+</sup> stem cells, inoculation with high-dose EBV ( $\sim 1 \times 10^3$  50% transformation dose [TD<sub>50</sub>]) resulted in the development of lymphoproliferative disorder, whereas inoculation with low-dose virus ( $< 1 \times 10^1$  TD<sub>50</sub>) tended to cause apparently asymptomatic persistent infection [15]. Immunological analyses of these mice demonstrated the presence of EBV-specific CD8<sup>+</sup> T cells that inhibit transformation of autologous B lymphocytes by the virus [16]. In the present study, we characterized histopathology of joint tissues obtained from EBV-infected humanized NOG mice and